CHARACTERIZATION OF THE PEROXISOMAL UBIQUITIN-CONJUGATING ENZYME 22 PROTEIN IN *ARABIDOPSIS THALIANA*

By

Ye Xu

A THESIS

Submitted to
Michigan State University
in partial fulfillment of requirements
for the degree of

Plant Biology – Master of Sciences

2014

ABSTRACT

CHARACTERIZATION OF THE PEROXISOMAL UBIQUITIN-CONJUGATING ENZYME 22 PROTEIN IN *ARABIDOPSIS THALIANA*

By

Ye Xu

Peroxisomes are small yet critical organelles that are present in nearly all eukaryotes. Peroxisomes house a broad range of metabolic and biochemical pathways that are vital for organismal development and metabolism. Unlike mitochondria and chloroplasts, which possess DNA transcription and protein translation machineries, almost all peroxisome matrix proteins are post-translationally targeted to peroxisomes after they are translated on free polyribosomes in the cytosol. Therefore, it is important to understand peroxisome protein import as well as degradation mechanisms. A number of proteins involved in peroxisome matrix protein import have been identified. However, our knowledge towards matrix protein degradation is still scarce. In this research, I explored the function of a newly identified component of the peroxisomal localized ubiquitin-proteasome system, i.e. ubiquitin-conjugating enzyme 22 (UBC22) in *Arabidopsis*. I provide evidence that AtUBC22 targets to peroxisomes through its C-terminal tri-peptide KRL>. Mutant analysis shows that UBC22 might act as a negative regulator of peroxisome IBA metabolism. UBC22 also has an effect on seed formation and seedling development. Homologous sequences of AtUBC22 that contain peroxisomal targeting signal type 1 are present in other plant species, indicating a plant-specific role of UBC22 in the peroxisome.

ACKNOWLEDGEMENTS

I would like to first give special thanks to my adviser Dr. Jianping Hu for letting me join this great lab and participating in the amazing world of peroxisome research. She has been super supportive and patient, and has constantly encouraged me to keep thinking, trying and exploring further. Without her, I would not have been able to finish this thesis.

I am also very grateful to have Dr. John Ohlrogge and Dr. Eva Farré as my committee members during the two years of study at MSU. Dr. Ohlrogge is a role model for me and has inspired me a lot, both in science and in life. He has always been so supportive and helpful even before he became my committee and I learnt a lot from him. Dr. Farré provided me with new perspectives in thinking about this project and gave me many critical suggestions on writing this thesis. Their support and advice have made me a better researcher.

I thank all Hu lab members, Dr. Navneet Kaur, Dr. Gaëlle Cassin, Ronghui Pan and Jiying Li. I would like to especially thank Navneet for her selfless help on my research and studies; she is a talented ‘teacher’ and great companion for every late night and weekends in the lab. Thanks also go to Ronghui Pan for being a good neighbor and helping me take care of my plants when I was on vacation.

I would like to thank many people in plant biology department and in PRL. Thanks to Dr. Alan Prather and Dr. Shin-Han Shiu for giving me the warmest help during the times I was feeling low. I sincere thank Dr. Weili Yang from Dr. Ohlrogge’s

lab for kindly helping me generate and analyze the fatty acid data. I also thank Dr. Giovanni Stefano on interesting discussion regarding confocal imaging.

I especially thank Yashiuan Lai for her company and support at every important moment during the past two years.

Lastly, I would like give my thanks to my parents and grandparents for their endless love and support.

TABLE OF CONTENTS

LIST OF TABLES

LIST OF FIGURES

KEY TO ABBREBIATIONS

β-gal	Beta-galactosidase
Δ	Deletion
35S	Cauliflower Mosaic Virus 35S promoter
AA	Amino acid
ABC	ATP binding cassette
ABRC	Arabidopsis Biological Resource Center
Acetyl-CoA	Acetyl coenzyme A
AD	Activation domain
Ala	Alanine
ATP	Adenosin-5'-Triphosphate
BD	DNA binding domain
BLAST	Basic Local Alignment Search Tool
C	Celsius
CAT	Catalase
CFP	Cyan fluorescent protein
Col-0	Columbia ecotype 0
C-terminal	Carboxy terminal
Cys	Cysteine
DsRed	Discosoma species red fluorescent protein
DUB	Deubiquitinase
ER	Endoplasmic reticulum
FA	Fatty acid

GFP	Green fluorescent protein
GOX	glycolate oxidase
H_2O_2	Hydrogen peroxide
IAA	Indole-3-acetic acid
IBA	Indole 3-butyric acid
IPTG	Isopropylthio-β-galactoside
JA	Jasmonic acid
JATI	Jasmonic acid triggered immunity
KDa	Kilo Dalton
Lys	Lysine
NM	Nanometer
N-terminal	Amino terminal
OPDA	12-oxo-phytodienoic acid
PBDs	Peroxisome biogenesis disorders
PEX	Peroxin
PIM	Peroxisome import machinery
PMPs	Peroxisome membrane proteins
PTMs	Post-translational modifications
PTS1	Peroxisomal targeting signal 1
PTS2	Peroxisomal targeting signal 2
RING	Really interesting new gene
RNS	Reactive nitrogen species
ROS	Reactive oxygen species

RuBisCO	Ribulose-1, 5-bisphosphate carboxylase/oxygenase
RuBP	Ribulose-1,5-bisphosphate
SD	Synthetic dropout
SD/-HUTL	SD media lacking histidine, uracil, tryptophan, and leucine
Ser	Serine
TAG	Triacylglycerols
Thr	Threonine
Tyr	Tyrosine
T-DNA	Transfer DNA
Ub	Ubiquitin
UBC	Ubiquitin conjugating enzyme
UBQ	Ubiquitin
UPS	Ubiquitin (Ub)-proteasome system
VLCFA	Very long chain fatty acids
WT	Wild-type
YFP	Yellow fluorescent protein

CHAPER 1

LITERATURE REVIEW

Peroxisomal Function, Biogenesis and Peroxisome-associated Proteolysis

1.1 Introduction

Peroxisomes are small, highly dynamic, and single-membrane-bounded organelles present in nearly all eukaryotes with the exception of mature erythrocytes and spermatozoa (Novikoff *et al.*, 1973). They are typically spherical, ranging from 0.1 to 1.5 micrometer in diameter. The number, morphology and function of peroxisomes, i.e. regular peroxisomes, glyoxysomes of plant seedlings and some fungi, glycosomes of trypanosomes, and Woronin bodies of filamentous fungi, vary dramatically among different cell types, tissues and species (Baker and Sparkes, 2005). Peroxisomes are involved in a wide variety of biological processes, and their metabolic and biochemical functions are critical in many aspects of eukaryotic development.

Some peroxisomal functions, such as the detoxification of hydrogen peroxide (H_2O_2) and fatty acid β-oxidation, are well conserved from yeast to man. As a versatile organelle, peroxisomes also contribute to a variety of other metabolic functions, some of which are lineage-specific. In mammals, peroxisomes carry enzymes involved in the synthesis of plasmalogens, cholesterol and bile acids as well as the oxidation of alcohols. Studies have shown that Alzheimer's disease might be associated with reduced level of brain plasmalogens (Rucktäschel *et al.*, 2011; Grimm *et al.*, 2011). Mutations in peroxins (PEX), i.e. proteins required for peroxisome biogenesis, lead to peroxisome biogenesis disorders (PBDs), the most severe of which (such as the Zellweger syndrome (ZS)) causes infant fatality (Fujiki *et al*., 2012; Faust *et al*., 2014). In plants, peroxisomes harbor diversified metabolic pathways and display various morphologies at different developmental stages and under various environmental conditions. In addition to lipid metabolism, the core enzymes of the β-oxidation pathway

are also involved in the synthesis of the plant hormone jasmonic acid (JA) and conversion of the protoauxin indole-3-butyric acid (IBA) to the active auxin indole-3-acetic acid (IAA). Furthermore, plant peroxisomes carry some unique functions, such as the glyoxylate cycle, photorespiration as well as nitrogen metabolism (Hu *et al.*, 2012). Fungal peroxisomes contain enzymes involved in the catabolism of unusual carbon and nitrogen sources, such as methanol, glycolate and spermidine. Yeast peroxisomes house important steps of lysine biosynthesis, and penicillin filamentous fungi generate penicillin in these organelles (Sibirny, 2012; Meijer *et al.*, 2010). Over the past decade, a growing amount of evidence indicates that defects in peroxisome biogenesis and metabolic functions cause fatality in early life of human and lethality to plant embryos, implicating the essential role of peroxisomes in these eukaryotes (Sparkes *et al.*, 2003; Lee and Raymond, 2013). Recent studies revealed novel functions of peroxisomes, such as their role in mammalian cell calcium homeostasis (Lasorsa *et al.*, 2008) and plant Vitamin K biosynthesis (Babujee *et al.*, 2010; Widhalm *et al.*, 2012).

Due to their sessile nature, plants need to deal with various environmental and developmental cues. Peroxisomes are key components of this process due to their functions such as degradation of very long chain fatty acids (VLCFA) to support seedling establishment of oilseed plants like *Arabidopsis*, biosynthesis of JA in response to wounding and pathogens, detoxification of harmful by-products such as reactive oxidative and nitrogen species (ROS and RNS, respectively), leaf senescence, and fruit maturation (Hu *et al.*, 2012; Linka *et al.*, 2008). Unlike mitochondria and chloroplasts that contain DNA transcription and protein translation machineries, almost all peroxisome proteins are post-translationally targeted to peroxisomes after they are

synthesized on free polyribosomes in the cytosol, with the exception of some peroxisome membrane proteins (PMPs) that are originated from the endoplasmic reticulum (ER) (Rucktäschel *et al.*, 2011). Proteins are imported into peroxisomes with the assistance of their targeting signals and peroxin (PEX) proteins. However, far less is known about how matrix proteins are degraded. There are many questions waiting for answers. For example, how and when do peroxisomes choose to degrade certain proteins? Does degradation of matrix proteins occur in peroxisomes or in the cytosol and what is the role of ubiquitination in this process?

1.2 Function of plant peroxisomes

The chief metabolic processes in peroxisomes that are crucial to plant development are fatty acid (FA) β-oxidation, generation of phytohormones JA and IAA, glyoxylate cycle in seedlings, and photorespiration. In addition, plant peroxisomes also contribute to other metabolic pathways, for instance biosynthesis of salicylic acid, biotin and isoprenoids, and metabolism of urate, polyamines, sulfite, and branched-chain amino acids (Kaur and Hu, 2009). Here, we will focus on the two major functions of peroxisome: ß-oxidation and photorespiration.

1.2.1 Peroxisomal ß-oxidation

Plant ß-oxidation solely occurs in peroxisomes, which contain a complete set of enzymes for the metabolism of fatty acids to acetyl coenzyme A (acetyl-CoA), as well as the conversion of IBA to active auxin IAA and 12-oxo-phytodienoic acid (OPDA) to JA (Hu *et al.*, 2012; Brown *et al.*, 2013).

1.2.1.1 Fatty acid ß-oxidation

Plant fatty acid ß-oxidation provides energy and carbon for post-germinative growth before plants establish photosynthesis, and it is also active throughout the life cycle of a plant. As the major components of plant oilseed reserve lipids, triacylglycerols (TAGs) are mobilized from oil bodies and imported into peroxisomes, where they are degraded to acyl-CoA and release acetyl-CoA during β-oxidation. The resulting acetyl-CoA pool is then further metabolized in the TCA cycle in the mitochondria to succinate and malate for gluconeogenesis or to citrate (Pracharoenwattana and Smith, 2008; Kunze *et al.*, 2006). Mutants that fail to break down storage fatty acids are unable to supply the necessary energy and carbon for the seedling to grow into a photosynthetic plant, and therefore typically show short primary roots and hypocotyls. This phenotype can be rescued by providing external sucrose. Recent studies show that peroxisome ß-oxidation also breaks down lipids during leaf senescence; in *Arabidopsis*, *Brachypodium* and switchgrass at least 80% of leaf fatty acids are degraded during senescence (Troncoso-Ponce *et al.*, 2013; Yang and Ohlrogge, 2009). However, *Arabidopsis* mutants of the core β-oxidation pathway enzymes, *acx1 acx2, lacs6 lacs7*, and *kat2,* which are defective in the breakdown of reserve oil in seeds during seed germination, do not show substantial deficiencies in the degradation of fatty acids during leaf senescence.

In *Arabidopsis*, fatty acids are transported into peroxisomes from oil bodies by the peroxisomal ATP binding cassette (ABC) transporter protein CTS/PXA1/PED3. After being imported into peroxisomes, saturated fatty acids (C18- C20) are activated to acyl-CoA by long chain acyl-CoA synthases 6 and 7 (LAC6 and LAC7) (Fulda *et al.*, 2002;

Hu *et al.*, 2012). Bioinformatics and genome analysis revealed 63 genes that encode ATP-dependent acyl-activating enzymes (AAEs) in *Arabidopsis*, and 17 members of this superfamily (including LAC6 and LAC7) carry a putative peroxisome targeting signal (PTS) (Shockey *et al.*, 2002; Sigrun Reumann *et al.*, 2004). In the ß-oxidation pathway, activated acyl-CoA are metabolized sequentially by acyl- CoA oxidase (ACX), the multifunctional proteins MFP2 or AIM1, and a thiolase PED1/KAT2 to produce acetyl-CoA and an acyl-CoA (C16 - C18) that is two Cs shorter. The shortened acyl-CoA is then further degraded through the same catalytic cycle in peroxisomes (Hu *et al.*, 2012). The activity of enzymes that are involved in fatty acid degradation varies depending on their affinity to substrates of various lengths, and therefore different enzymes participate at different stages in the pathway. For instances, AIM1 prefers short-chain substrates while MFP2 has higher activity towards long-chain acyl-CoAs (Arent *et al.*, 2010; Rylott *et al.*, 2006). In *Arabidopsis* and other plants, acetyl-CoA can be converted to succinate and malate, which will be later used for gluconeogenesis, or it can also be converted to citrate which then is exported to mitochondria (Kunze *et al.*, 2006; Pracharoenwattana and Smith, 2008).

1.2.1.2 Conversion of IBA to IAA

IAA is the major form of plant auxin. As a critical plant hormone, IAA regulates a variety of developmental events and environmental responses through the control of cell division and expansion in lateral root initiation, root and stem elongation, and leaf expansion, *etc.* (Davies, 2010). IBA is also a natural auxin, which is structurally similar to IAA but has two additional methylene groups in the side chain. Like IAA, exogenous IBA can inhibit primary root elongation and induces lateral root formation (Zolman *et al.*,

2000). IBA can be converted to IAA in plant peroxisomes, and IAA can also be converted back to IBA as a storage form to maintain IAA homeostasis (Ludwig-Muller *et al.*, 1994).

IBA fulfills its bioactivity mainly through its conversion to IAA. Mutants that are defective in this event fail or partially fail to convert IBA into IAA and thus their seedlings are resistant to exogenous IBA – i.e. showing reduced response to IBA's inhibition on primary root elongation and induction of lateral root formation. Several mutants defective in fatty acids ß-oxidation show IBA resistant phenotypes. Some IBA resistant mutants are sucrose dependent during early developmental stages, indicating that the four-carbon side chain in IBA can be modified to the two-carbon side chain in IAA in a ß-oxidation pathway parallel to fatty acid ß-oxidation in peroxisomes (Zolman and Bartel, 2004; Zolman *et al.*, 2001). IBA is imported into peroxisomes, activated to IBA-CoA, and further converted to IAA-CoA through a pathway similar to fatty acid ß-oxidation. The *pxa1* mutant shows both sucrose dependent and IBA resistant phenotypes, indicating that other than importing fatty acids, PXA1 might also contribute to IBA import. Some fatty acid ß-oxidation pathway mutants like *acxs, aim1 and ped1/kat2* are also resistant to exogenous IBA, while *ibr1, ibr3, ibr10* only show IBA resistant phenotypes, suggesting that the latter mutants might only be defective in IBA-CoA ß-oxidation and therefore the corresponding protein products are specific for the IBA pathway.

1.2.1.3 JA biosynthesis

Plants are the nutritional sources for a variety of living things including herbivores,

microorganisms and pathogens. In order to survive, plants synthesize JA to trigger downstream chemical defense compounds to repel plant consumers. JA is an important plant hormone that regulates plant growth and development including nectar accumulation, leaf senescence and abscission, flower development, *etc.* It is also involved in biotic and abiotic stress responses, like the pathogen- or wound-induced multistage process called JA-triggered immunity (JATI) (Campos *et al.*, 2014; He and Gan, 2002; Radhika *et al.*, 2010).

The production of active JA is initiated in plastids, where the polyunsaturated fatty acid C18 precursor linolenic acid (LA) is converted to the lipid intermediate 12-oxo-phytodienoic acid (OPDA), which is further transported to peroxisomes and converted to JA through ß-oxidation. JA is then released to the cytosol and conjugated with Ile to form JA-Ile, which presumably diffuses into the nucleus and binds to the JAZ (JAsmonate ZIM domain) repressors and targets them to degradation via the ubiquitin-dependent protein degradation pathway. Degradation of JAZ proteins releases the repression on transcription factors (TFs) for JA-response genes (Campos *et al.*, 2014). In *Arabidopsis*, the peroxisomal steps of this pathway start from the import of OPDA by PXA1. OPDA is then reduced by a flavin-dependent 12-oxophytodienoate reductase (OPR), OPR3, to 3-oxo-2-(20-[Z]-pentenyl)-cyclopentane-1-octanoic acid (OPC-8) (Breithaupt *et al.*, 2009). After OPC-8 is activated by an OPC-8:0 CoA ligase 1 (OPCL1) and forms OPC8:0-CoA (Koo *et al.*, 2006), OPC8:0-CoA goes through three rounds of ß-oxidation with each round removing two carbon units, to finally form JA-CoA. Similar to fatty acid ß-oxidation, this process involves ACX (ACX1 and ACX5), AIM1 and KAT2 (Castillo *et al.*, 2004; Afitlhile *et al.*, 2005; Vrebalov *et al.*, 2005; Schilmiller *et al.*, 2007).

After ß -oxidation, JA-CoA is hydrolyzed by a currently unknown thiosterase to release JA, which is then exported from peroxisomes into the cytosol for further modifications.

1.2.2 Peroxisome and Photorespiration

Photorespiration is a process that enables photosynthetic organisms to recycle carbon from the oxygenase reaction catalyzed by ribulose-1, 5-bisphosphate carboxylase/oxygenase (Rubisco). This procedure produces an inevitable toxic reactive oxygen species (ROS) by-product, hydrogen peroxide (H_2O_2), which then can be detoxified by a peroxisomal exclusive antioxidant catalase (CAT) (Apel and Hirt, 2004). Besides H_2O_2, peroxisomes also produce other superoxide-radicals and nitric oxide (NO•), which are known cellular signals that participate in a variety of intra- and inter-cellular communication (Corpas *et al.*, 2001).

In 1920, Warburg first reported that O_2 can inhibit photosynthesis. Later studies showed that lowering O_2 concentration to 2% can lead to a 20-30% increase in biomass and yield in plants, while when O_2 concentration was above the atmospheric level, photosynthesis was severely reduced (Maurino and Peterhansel, 2010). Current explanation of how O_2 inhibits photosynthesis is that Rubisco could catalyze both the oxygenation and carboxylation reactions with Ribulose-1, 5-bisphosphate (RuBP), depending on the $[CO_2]/[O_2]$ ratio in the chloroplast and around Rubisco (Moroney *et al.*, 2013). Carboxylation of RuBP produces two molecules of 3-phosphoglycerate (3-PGA), while oxygenation synthesizes one molecule of 3-PGA and one molecule of 2-phosphoglycolate (2-PG). After dephosphorylation, 2-PG enters the photorespiratory pathway in which 75% of its carbon returns as 3-PGA to the Calvin–Benson–Bassham

cycle (CBB cycle) while the rest 25% of the carbon is lost as CO_2. When O_2 concentration around Rubisco increases, Rubisco's affinity for CO_2 decreases and reacts more with O_2 to generate 2-PG, thus carbon, biomass and yield are lost in plants (Moroney *et al.*, 2013). Due to this property, the photorespiration pathway is viewed as a major target for crop yield improvement (Hu *et al.*, 2012).

To sum up the photorespiration process, 2-PG is first dephosphorylated in the chloroplasts by phosphoglycolate phosphatase (PGLP) to glycolate, which is then transported to peroxisomes where it is oxidized by glycolate oxidase (GOX) to equimolar amounts of glyoxylate and H_2O_2. Glyoxylate is further transaminated by glutamate–glyoxylate amino- transferase (GGAT) to glycine, which is transported to mitochondria. In mitochondria, glycine decarboxylase decomposes two molecules of glycine into one molecule of serine and releases one molecule each of CO_2 and ammonia (NH_4^+). Serine is then transferred back to peroxisomes and metabolized by a serine-glyoxylate aminotransferase (SGT) to hydroxypyruvate, which is further converted to glycerate by hydroxypyruvate reductase (HPR). Glycerate is transported to chloroplasts where it is phosphorylated by glycerate kinase (GLYK) to 3-PGA, which then reenters the CBB cycle (Hu *et al.*, 2012; Maurino and Peterhansel, 2010; Moroney *et al.*, 2013).

1.3 Peroxisomal protein remodeling and proteases

1.3.1 Peroxisomal matrix protein import

Despite their diversified functions and morphologies, all types of peroxisomes share an essentially conserved matrix protein import system. As peroxisomes contain

neither genetic material nor transcription/translation machineries, all of its matrix proteins are encoded in the nucleus, translated on free polyribosomes in the cytosol and then targeted to peroxisomes (Léon et al., 2006b). In *Arabidopsis thaliana*, approximately 280 proteins were predicted to target to the peroxisomal matrix (Reumann *et al.*, 2004). In addition, peroxisomes are capable of importing fully folded or even oligomeric and co-factor bound proteins, distinguishing it from other organelles in their protein import mechanism (Léon et al., 2006a). Different from the origin of matrix proteins, some peroxisome membrane proteins originate in the ER. Examples include cottonseed (*Gossypium hirsutum*) and pumpkin (*Cucurbita maxima*) ascorbate peroxidase (APX) and *Arabidopsis thaliana* PEX16 (Yamaguchi *et al.*, 1995; Bunkelmann and Trelease, 1996; Karnik and Trelease, 2005; Nito *et al.*, 2007).

The peroxisome protein import process for matrix proteins can be divided into four steps (Figure 1.1): 1) the matrix protein is recognized by the receptor in the cytosol; 2) the receptor-cargo complex docks to the peroxisome membrane; 3) the cargo is imported into the peroxisome matrix through the membrane and released into the matrix; and 4) the receptor returns to the cytosol for recycling or degradation (Hasan *et al.*, 2013). At present, 19 out of the 34 PEX genes discovered have been demonstrated to be directly involved in peroxisomal matrix protein import.

Step 1: Cargo-recognition

Following translation, nascent peroxisomal matrix proteins are recognized by receptors through the peroxisomal targeting signal (PTS), which is either located at the C-terminus (PTS1, peroxisomal targeting signal type 1) or the N-terminus (PTS2) of

matrix proteins. The majority of the matrix proteins possess PTS1, a tripeptide at the C-terminal end of the protein. A typical PTS1 is usually comprised of Ser-Lys-Leu (SKL) or variants that fit the consensus (S/A/C)-(K/R/H)-(L/A). PTS1 sequences are recognized by a conserved cytoplasmic receptor PEX5. PEX5 contains two functional domains: a natively unfolded N-terminal peroxisome docking domain and a C-terminal domain, which contains tetratricopeptide repeats (TPRs) that allow it to recognize the PTS1-sequence (Carvalho *et al.*, 2006). Recent studies reported that the conformation of unloaded PTS1-receptor changes upon binding with cargo, allowing the receptors to transfer into a docking competent state (Shiozawa *et al.*, 2009; Stanley *et al.*, 2006; Fodor *et al.*, 2012).

The minority of matrix proteins possesses PTS2. In *Arabidopsis thaliana,* about 220 proteins are predicted to contain a putative PTS1, while only 60 proteins carry PTS2 (Lingner *et al.*, 2011). The usage of PTS2 for peroxisome matrix protein import varies among species. In plants, around one third of peroxisome matrix proteins contain the PTS2 motif (Reumann *et al.*, 2009). In contrast, in mammals only a few proteins use this pathway, in yeast *Saccharomyces cerevisiae* three proteins have been identified to harbor a PTS2 sequence (Grunau *et al.*, 2009; Jung *et al.*, 2010), and in some species such as *Caenorhabditis elegans* and *Drosophila melanogaster* the PTS2 pathway is completely absent (Motley *et al.*, 2000; Faust *et al.*, 2012). PTS2 is a nonapeptide within the first 20 amino acids of a matrix protein, and possesses the consensus sequence (RK)-(LVIQ)-XX-(LVIHQ)-(LSGAK)-X-(HQ)-(LAF) that is recognized by the tryptophan-aspartic acid (WD) repeats motif of the soluble receptor PEX7 (Lazarow, 2006; Petriv *et al.*, 2004; Rucktäschel *et al.*, 2011).

Some proteins have been reported to be imported through a non-classical pathway. The *Trypanosoma brucei* glycosomal enzyme triosephosphate isomerase (TPI) and the pumpkin catalase CAT1 both contain internal PTS motifs (Oshima *et al.*, 2008; Galland *et al.*, 2010). *S. cerevisiae* enoyl-CoA isomerases Eci1p and Dci1p and mammalian Cu/Zn superoxide dismutase are imported by association with another canonical PTS-containing cargo protein through a manner called “piggy-back import” (Islinger *et al.*, 2009; Yang *et al.*, 2001). Some proteins are imported through a “non-PTS import” method. For example, *S. cerevisiae* acyl-CoA oxidase and *H. polymorpha* alcohol oxidase interact directly with Pex5’s N-terminal region without possessing a PTS sequence (Gunkel *et al.*, 2004; Klein *et al.*, 2002).

Step 2: Receptor-cargo complex docking

After the receptor-cargo complex is formed in the cytosol, it associates with the peroxisomal membrane via a docking complex. This docking complex consists of PEX13 and PEX14 in plants, and in fungi it contains the peroxin Pex17p as well (Kiel *et al.*, 2006). Yeast Pex13p is an integral membrane protein that exposes both its C- and N-termini to the cytosol and binds to Pex14p via its SH3 domain and an intraperoxisomal binding site (Schell-steven *et al.*, 2005; Pires *et al.*, 2003). Pex13p also binds to Pex5p via its C-terminal Src-homology-3 (SH3) domain in yeasts *S. cerevisiae* and *P. pastoris* (Williams and Distel, 2006) and with Pex7p via its N-terminal domain in *S. cerevisiae* (Stein *et al.*, 2002). Pex14p forms a complex with Pex13p through its proline-rich segment and it binds to both PTS receptors (Niederhoff *et al.*, 2005). PEX14 was described as an integral membrane protein in *Arabidopsis thaliana*, while in some other species, it was shown to be a peripheral protein (Azevedo and Schliebs, 2006).

Yeast Pex17p is a peripheral membrane protein, and its function in the docking complex is still unknown (Huhse *et al*., 1998).

Unlike PEX5, PEX7 itself is unable to complete all steps for matrix protein import, so it needs auxiliary proteins. In plants, PEX5 is required for PEX7 to correctly bind to the docking complex. In mammals and rice, a long isoform (Pex5L) serves as the PEX7 co-receptor, in most yeasts and fungi the co-receptor is Pex20p, and in *S. cerevisiae* the redundant proteins Pex18p and Pex21p act as the co-receptor (Schliebs and Kunau, 2006).

Step 3: Cargo translocation and releasing

The receptor-cargo complex is translocated into peroxisomes in a folded or even oligomerized form and then released into the peroxisomal matrix. However, the mechanism behind this process is still unclear. Currently several hypotheses have been proposed. In yeast *S. cerevisiae*, Pex5p and Pex14p are able to form a dynamic translocation pore for the receptor-cargo complex to pass through. Evidence show that this pore can open up to 9 nm in diameter, and even gold particles fused with a PTS can pass through the membrane (Walton, 1996; Meinecke *et al*., 2010). Besides, this process might also be facilitated by a post docking protein complex, the RING (really interesting new gene)-finger complex that contains the peroxisomal membrane proteins Pex2p, Pex10p and Pex12p (Platta and Erdmann, 2007). Recent studies demonstrate that RING proteins have E3 ligase activities in *S. cerevisiae* and *Arabidopsis thaliana.* Lack or reduction of the expression of any of these RING peroxins remarkably decreases the import efficiency for both PTS1- and PTS2-containing proteins even after

docking, and knocking out *PEX2, PEX10* or *PEX12* in *Arabidopsis thaliana* causes embryo lethality (Kaur *et al.*, 2013; Hu *et al.*, 2002; Embryogenesis *et al.*, 2014; Schumann *et al.*, 2003; Fan *et al.*, 2005).

After the receptor-cargo complex is translocated into the peroxisomal lumen, the cargo is unloaded through a still unknown mechanism. In plants and mammals, PTS2 on the imported cargo is proteolytically removed after import. In mammalian cells, Tysnd1 was demonstrated to be responsible for removing the sequence peptides from PTS2 proteins involved in β-oxidation of fatty acids (Okumoto *et al.*, 2011). Pex8p of *H. polymorpha*, an intra-peroxisomal peripheral membrane protein that contains both PTS1 and PTS2, has been proposed to play a role in cargo releasing by facilitating the disassociation of PTS1 peptides from Pex5p *in vitro* (Wang *et al.*, 2003). A recent study in *P. pastoris* shows that Pex8p aids in cargo release by assisting Pex5p transfer from a redox-regulated oligomer to a dimer (Ma *et al.*, 2013). Furthermore, Pex8p is necessary for the correct binding of the docking complex (Pex13p, Pex14p and Pex17p) to the peroxisomal RING-finger complex (Pex2p, Pex10p and Pex12p) to form the "importomer" (Agne *et al.*, 2003). However, Pex8p seems to be exclusively present in yeast and absent in all higher eukaryotes (Kiel *et al.*, 2006). Another peroxin, mammalian PEX14, has been shown to be involved in this process by helping to release the cargo from PEX5 (Freitas *et al.*, 2011).

Final step: Receptor recycling and degradation.

Following cargo release, receptors are dislocated from the peroxisomal matrix and back to the cytosol for either degradation or recycling through an ubiquitin-

dependent manner. This process involves a set of sub-complexes. In contrast to the import pathway, which is ATP-independent, the export procedure demands ATP for two different steps, ubiquitination and export. In yeast, the necessary machinery is comprised of the RING-finger complex (Pex2p, Pex10p and Pex12p), which displays ubiquitin protein ligase (E3) activity, the ubiquitin-conjugating enzyme (E2) Pex4p together with its membrane anchor Pex22p, and two AAA-protein family (ATPases Associated with diverse cellular Activities family) members Pex1p and Pex6p (Grou *et al*., 2009a). Ubiquitination provides the export signal for the receptor and allows it to be recognized by the dislocation machinery, and this requirement seems to be conserved in all eukaryotes (Okumoto et al., 2011b). Pex5p monoubiquitination depends on the RING complex member Pex12p (E3) and Pex4p (E2). Then ubiquitinated Pex5p is dislocated to cytosol via Pex1p and Pex6p (Grou et al., 2009a). In mammalian cells, instead of PEX4 and PEX22, UbcH5a, UbcH5b and UbcH5c catalyze the monoubiquitination step (Grou *et al.*, 2008). Pex1p and Pex6p are anchored to the membrane via an integral peroxisomal membrane protein, i.e. Pex15p in yeast, Pex26 in mammals and APEM9 in plants. Pex6p first binds to Pex15p, then recruits Pex1p through an ATP-dependent manner (Goto *et al.*, 2011; Matsumoto *et al.*, 2003; Birschmann *et al.*, 2003). Recent evidence shows that this AAA complex provides the driving force for the export of Pex5p (Platta *et al.*, 2005). It has been hypothesizes that the receptor export machinery might function as a molecular motor in both receptor dislocation and protein translocation (Platta *et al.*, 2014).

Once or shortly after the receptor has been exported to the cytosol, the mono-ubiquitin moiety on the receptor is removed through two ways. In the non-enzymatic

way, the nucleophilic attack of glutathione cleaves the thioester bond between Pex5p and ubiquitin. In the enzymatic way, the mono-ubiquitin on PEX5 is hydrolysed by USP9X in mammals and Ubp15p in yeast (Grou et al., 2009b; Debelyy et al., 2011).

PEX5 is mono-ubiquitinated on the conserved cysteine residue for recycling. However, when the recycling pathway is impaired, Pex5p is polyubiquitinated on lysine residues, resulting in its degradation via the 26S proteasome system (Kiel *et al.*, 2004). In *S. cerevisiae,* ubiquitin- conjugating enzyme (E2) Ubc4p, Ubc5p and Ubc1p have been demonstrated to be involved in the polyubiquitination of Pex5p (Kragt *et al.*, 2005; Kiel *et al.*, 2004). Ubiquitination also affects the PTS2 pathway. The yeast *S. cerevisiae* PTS2 co-receptor Pex18p and the *P. pastoris* PTS2 co-receptor Pex20p are ubiquitinated at the peroxisome membrane. In *P. pastoris,* Pex4p is essential for the mono- and polyubiquitination of Pex20p (Liu and Subramani, 2013). Due to lack of a corresponding protease, yeast is unable to cut off the PTS2 signal from the cargo following its import into the peroxisomal lumen (Helm *et al.*, 2007). So far, our knowledge about the PEX7 pathway and whether PEX7? Is ubiquitinated in this process is still lacking.

1.3.2 Peroxisomal protein degradation

For some organelles, protein export is a vital process to guarantee the normal function of the organelle. Failure to export certain proteins from the organelle matrix at a specific stage or blocking the export of misfolded proteins may be detrimental to the organelle and ultimately lead to disease. ER exports its misfolded membrane and matrix proteins to the cytosol for degradation through the endoplasmic reticulum associated

degradation (ERAD) pathway. Likewise, mitochondria export damaged proteins through mitochondrial associated degradation (MAD). Dysfunction of any of these pathways causes severe diseases. For example, in human, failure to secrete ATZ (Alpha-1 antitrypsin Z) from ER to the blood leads to chronic liver inflammation in children and hepato-cellular carcinoma later in life (Perlmutter, 2006). Mitochondrial loss of function mutations in protein degradation lead to parkinson disease (Heo and Rutter, 2011). All those examples underscore the importance of protein export in maintaining organelle functions. However, the export mechanism and the role of cysteine-ubiquitination in this process are poorly understood.

Several peroxisomal proteases have been reported. *Arabidopsis* DEG15 and its mammalian homolog trypsin containing domain 1 (TYSND1) are ATP-dependent ser proteases, functioning as signal peptidases that are able to cut off the PTS signal from imported matrix proteins (Kurochkin *et al.*, 2007; Novikoff *et al.*, 1973; Perlmutter, 2006). *Arabidopsis* plants lacking DEG15 display mild IBA resistant phenotype and fail to process several PTS2-containing proteins (Schuhmann *et al.*, 2008). Besides, all currently identified Tysnd1 substrates are involved in peroxisomal β-oxidation, prompting a model in which Tysnd1 promotes the assembly of peroxisomal enzymes into a supramolecular complex thus accelerates the β-oxidation process (Kurochkin *et al.*, 2007).

Plant peroxisomes also possess a quality control system that involves a Long Form Radiation Sensitive (Lon) protease family member LON2. Similar to DEG15, LON proteases are also ATP-dependent proteins, which have been demonstrated to play a crucial role in the degradation of damaged and oxidized proteins in human(Bota and

Davies, 2002). In plants, LON isoforms are targeted to chloroplasts, mitochondria, and peroxisomes. Its peroxisomal isoform LON2 is assumed to participate in peroxisomal quality control processes, and has been shown to facilitate the sustained import of matrix proteins in *Arabidopsis* (Bartoszewska *et al.*, 2012). This result indicates the importance of intra-peroxisomal proteolysis in maintaining the peroxisome import system (Lingard and Bartel, 2009). Suppressor screens of the *Arabidopsis lon2* mutants found several independent mutations that can fully suppress *lon2* defects. The genes involved include the autophagy genes *ATG2, ATG3* and *ATG7,* indicating the possible existence of pexophagy (peroxisomal autophagy) in plants (Farmer *et al.*, 2013). In addition, LON2 plays a role in matrix protein turnover. After ~4 days of germination, *Arabidopsis* seedlings no longer rely on stored fatty acids to provide energy for growth and have established into photosynthetic plants. During this transition, enzymes of the glyoxylate cycle, such as isocitrate lyase (ICL) and malate synthase (MLS), are degraded. A new set of proteins involved in the photorespiratory pathway, like hydroxypyruvate reductase1 (HPR1) (Williams, 2014), arise. Surprisingly, in *Arabidopsis lon2* mutants, glyoxylate enzymes are degraded more quickly than in the wild type, rather than more slowly as expected, indicating that pexophagy may be accelerated when the LON2 protease level is decreased (Bartel *et al.*, 2014).

Up to date, two models have been proposed to explain the transition of peroxisomes from seed peroxisomes (glyoxysomes) to leaf peroxisomes. One model suggested that glyoxysomes directly substitute protein content and become leaf peroxisomes to meet the metabolic requirements of the plants. The other model states that there are two types of peroxisomes, one containing enzymes for glyoxysomal

metabolism and the other for photorespiration. When a plant becomes photosynthetic, glyoxysomes are degraded and seedlings start to generate the later type of peroxisomes (Burke and Trelease, 1975). Studies on pumpkin (*Cucurbita pepo*), watermelon (*Citrullis vulgaris*), and cucumber (*Cucumis sativus*) via immunocytochemistry support the first model, in which glyoxysomes are modified to become leaf peroxisomes without *de novo* biogenesis of leaf peroxisomes (Sautter, 1986; Nishimura *et al.*, 1986; Titus and Becker, 1985).

A recent study revealed the role of a cysteine protease RESPONSE TO DROUGHT21A-LIKE1 in *Arabidopsis* germination, β-oxidation, and growth (Quan *et al.*, 2013). Several peroxisomal proteases have also been discovered through proteomics and bioinformatics, and their functions are waiting to be uncovered.

1.4 Aims of the thesis research

Our understanding of peroxisomes advanced greatly during the past twenty years, yet many aspects about this important organelle are still largely unknown. This thesis aims to contribute to the understanding the proteolytic processes inside peroxisomes and the role of ubiquitination in peroxisomal metabolism and biochemical functions in *Arabidopsis*. In Chapter 2, I will focus on the characterization of the peroxisomal associated ubiquitin-proteasome system in *Arabidopsis* by studying a novel peroxisomal localized protein, ubiquitin-conjugating enzyme 22 (UBC22).

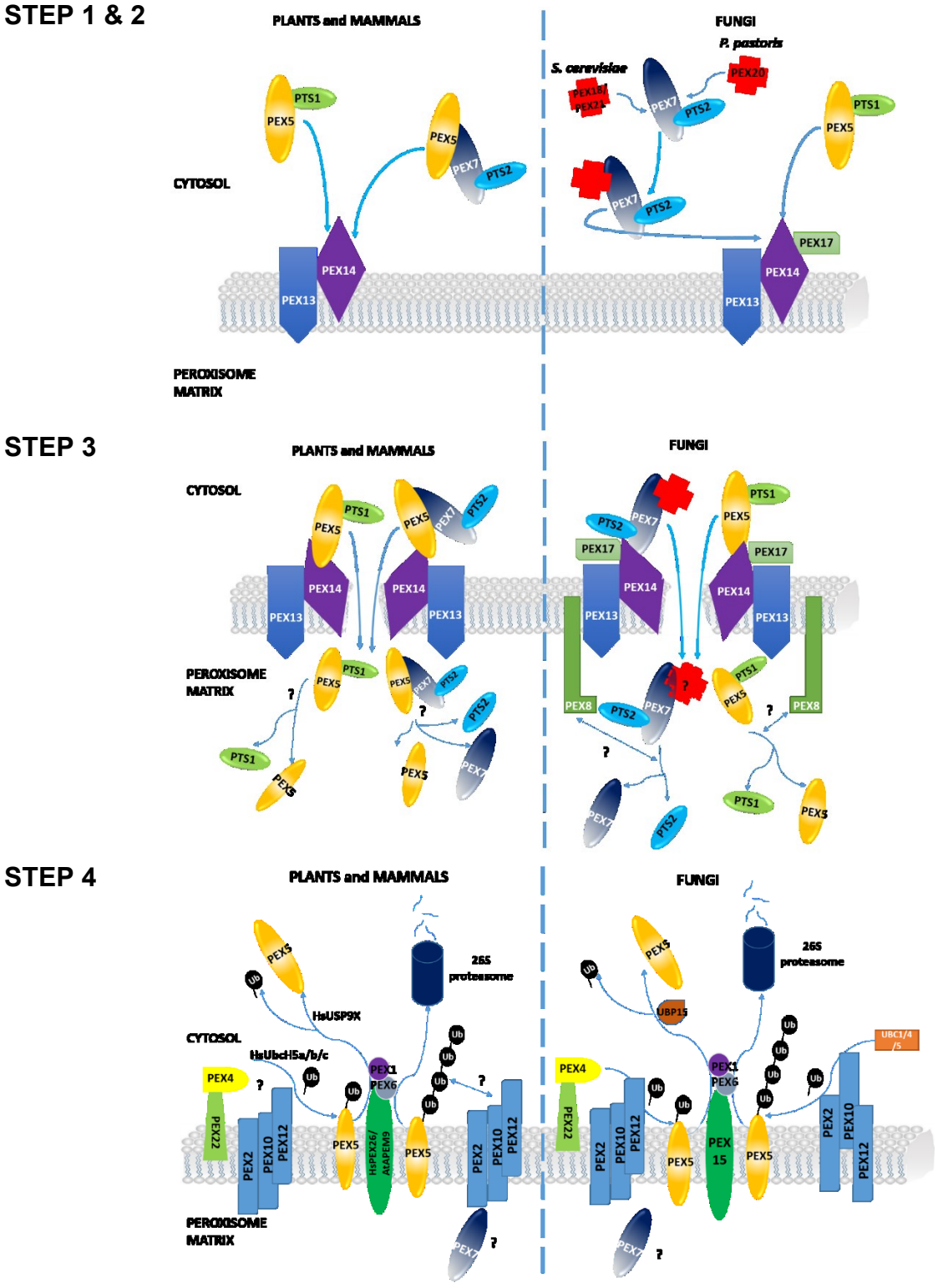

Figure 1.1. Model for peroxisome matrix protein import machinery.

Figure 1.1 cont'd

STEP1 & 2. Cargo-recognition and docking.
In the cytosol, peroxisomal matrix proteins harboring a PTS1 or PTS2 are recognized by the import receptors PEX5 and PEX7 respectively. Then the loaded receptors target to the docking complex (PEX13 and PEX14, and in fungi it contains the peroxin Pex17p as well) on the peroxisomal membrane. Unlike PEX5, PEX7 itself is unable to target to the docking complex and needs auxiliary proteins. In plants, PEX5 is required for PEX7 to correctly bind to the docking complex. In mammals and rice, a long isoform (Pex5L) serves as the PEX7 co-receptor, in most yeasts and fungi the co-receptor is Pex20p, and in *S. cerevisiae* the redundant proteins Pex18p and Pex21p act as the co-receptor.

STEP3. Cargo translocation and releasing.
It is assumed that the interaction between PEX5 and PEX14 forms a transient channel in the peroxisome membrane that allows the import of the cargo-loaded receptor complex to enter the peroxisome. In fungi, an intraperoxisomal protein Pex8p might be involved in cargo releasing. In plants and mammals, this mechanism is unknown.

STEP4. Receptor recycling and degradation.

Receptors are dislocated to the cytosol for either degradation or recycling through an ubiquitin-dependent manner. This process requires ATP for ubiquitination and export, and involves a set of sub-complexes. In yeast, this machinery is comprised of the RING-finger complex (Pex2p, Pex10p and Pex12p) that displays ubiquitin-protein ligase (E3) activity, ubiquitin-conjugating enzyme (E2) Pex4p together with its membrane anchor Pex22p, and two AAA-protein Pex1p and Pex6p. Ubiquitination provides the export signal for the receptor and allows it to be recognized by the dislocation machinery. Pex5p monoubiquitination depends on Pex12p (E3) and Pex4p (E2). Pex5p polyubiquitination depends on Ubc4p (E2) and the RING proteins Pex2p and Pex10p. Ubiquitinated Pex5p is dislocated to cytosol via Pex1p and Pex6p. In mammalian cells, UbcH5a, UbcH5b and UbcH5c catalyze the monoubiquitination step. Pex1p and Pex6p are anchored to the membrane via an integral peroxisomal membrane protein, i.e. Pex15p in yeast, Pex26 in mammals and APEM9 in plants. Pex6p first binds to Pex15p, then recruits Pex1p through an ATP-dependent manner. AAA complex provides the driving force for the export of Pex5p. Once or shortly after the receptor has been exported to the cytosol, the mono-ubiquitin moiety on the receptor is removed

REFERENCES

REFERENCES

Afitlhile, M.M., Fukushige, H., Nishimura, M., and Hildebrand, D.F. (2005). A defect in glyoxysomal fatty acid beta-oxidation reduces jasmonic acid accumulation in Arabidopsis. Plant Physiol. Biochem. **43**: 603–9.

Agne, B., Meindl, N.M., Niederhoff, K., Einwächter, H., Rehling, P., Sickmann, A., Meyer, H.E., Girzalsky, W., and Kunau, W.H. (2003). Pex8p: an intraperoxisomal organizer of the peroxisomal import machinery. Mol. Cell **11**: 635–46.

Apel, K. and Hirt, H. (2004). Reactive oxygen species: metabolism, oxidative stress, and signal transduction. Annu. Rev. Plant Biol. **55**: 373–99.

Arent, S., Christensen, C.E., Pye, V.E., Nørgaard, A., and Henriksen, A. (2010). The multifunctional protein in peroxisomal beta-oxidation: structure and substrate specificity of the Arabidopsis thaliana protein MFP2. J. Biol. Chem. **285**: 24066–77.

Azevedo, J.E. and Schliebs, W. (2006). Pex14p, more than just a docking protein. Biochim. Biophys. Acta **1763**: 1574–84.

Babujee, L., Wurtz, V., Ma, C., Lueder, F., Soni, P., van Dorsselaer, A., and Reumann, S. (2010). The proteome map of spinach leaf peroxisomes indicates partial compartmentalization of phylloquinone (vitamin K1) biosynthesis in plant peroxisomes. J. Exp. Bot. **61**: 1441–53.

Baker, A. and Sparkes, I.A. (2005). Peroxisome protein import: some answers, more questions. Curr. Opin. Plant Biol. **8**: 640–7.

Bartel, B., Farmer, L.M., Rinaldi, M.A., Young, P.G., Danan, C.H., and Burkhart, S.E. (2014). Mutation of the Arabidopsis LON2 peroxisomal protease enhances perophagy. Autophagy **10**: 518–519.

Bartoszewska, M., Williams, C., Kikhney, A., Opaliński, Ł., van Roermund, C.W.T., de Boer, R., Veenhuis, M., and van der Klei, I.J. (2012). Peroxisomal proteostasis involves a Lon family protein that functions as protease and chaperone. J. Biol. Chem. **287**: 27380–95.

Birschmann, I., Stroobants, A.K., and Berg, M. Van Den (2003). Pex15p of Saccharomyces cerevisiae Provides a Molecular Basis for Recruitment of the AAA Peroxin Pex6p to Peroxisomal Membranes. Mol. Biol. Cell **14**: 2226–2236.

Bota, D. a and Davies, K.J. a (2002). Lon protease preferentially degrades oxidized mitochondrial aconitase by an ATP-stimulated mechanism. Nat. Cell Biol. **4**: 674–80.

Breithaupt, C., Kurzbauer, R., Schaller, F., Stintzi, A., Schaller, A., Huber, R., Macheroux, P., and Clausen, T. (2009). Structural basis of substrate specificity of plant 12-oxophytodienoate reductases. J. Mol. Biol. **392**: 1266–77.

Brown, L., Larson, T.R., Graham, I.A., Hawes, C., Paudyal, R., Warriner, S.L., and Baker, A. (2013). Rapid report An inhibitor of oil body mobilization in Arabidopsis. New Phytol.: 641–649.

Bunkelmann, J.R. and Trelease, R.N. (1996). Ascorbate Peroxidase A Prominent Membrane Protein in Oilseed Glyoxysomes. Plant Physiol. **110**: 589–598.

Burke, J.J. and Trelease, R.N. (1975). Cytochemical Demonstration of Malate Synthase and Glycolate. Plant Physiol. **56**: 710–717.

Campos, M.L., Kang, J.-H., and Howe, G. a (2014). Jasmonate-Triggered Plant Immunity. J. Chem. Ecol. **online**.

Carvalho, A.F., Costa-Rodrigues, J., Correia, I., Costa Pessoa, J., Faria, T.Q., Martins, C.L., Fransen, M., Sá-Miranda, C., and Azevedo, J.E. (2006). The N-terminal half of the peroxisomal cycling receptor Pex5p is a natively unfolded domain. J. Mol. Biol. **356**: 864–75.

Castillo, M.C., Martinez, C., Buchala, A., Metraux, J.-P., and Leon, J. (2004). Gene-Specific Involvement of b -Oxidation in Wound-Activated Responses in Arabidopsis 1. Plant Physiol. **135**: 85–94.

Corpas, F.J., Barroso, J.B., and del Río, L. a (2001). Peroxisomes as a source of reactive oxygen species and nitric oxide signal molecules in plant cells. Trends Plant Sci. **6**: 145–50.

Davies, P.J. (2010). Plant Hormones: Biosyn- thesis, Signal Transduction, Action! 3rd ed. P.J. Davies, ed (Kluwer Academic Publishers, Dordrecht, The Netherlands).

Debelyy, M.O., Platta, H.W., Saffian, D., Hensel, A., Thoms, S., Meyer, H.E., Warscheid, B., Girzalsky, W., and Erdmann, R. (2011). Ubp15p, a ubiquitin hydrolase associated with the peroxisomal export machinery. J. Biol. Chem. **286**: 28223–34.

Embryogenesis, P., Sparkes, I.A., Brandizzi, F., Slocombe, S.P., El-shami, M., Hawes, C., and Baker, A. (2014). An Arabidopsis pex10 Null Mutant Is Embryo Lethal , Implicating Peroxisomes in an Essential Role during. Plant Physiol. **133**: 1809–1819.

Fan, J., Quan, S., Orth, T., Awai, C., Chory, J., and Hu, J. (2005). The Arabidopsis PEX12 Gene Is Required for Peroxisome Biogenesis and Is Essential for Development. Plant Physiol. **139**: 231–239.

Farmer, L.M., Rinaldi, M. a, Young, P.G., Danan, C.H., Burkhart, S.E., and Bartel, B. (2013). Disrupting autophagy restores peroxisome function to an Arabidopsis lon2 mutant and reveals a role for the LON2 protease in peroxisomal matrix protein degradation. Plant Cell **25**: 4085–100.

Faust, J.E., Manisundaram, A., Ivanova, P.T., Milne, S.B., Summerville, J.B., Brown, H.A., Wangler, M., Stern, M., and McNew, J. a (2014). Peroxisomes Are Required for Lipid Metabolism and Muscle Function in Drosophila melanogaster. PLoS One **9**: e100213.

Faust, J.E., Verma, A., Peng, C., and McNew, J.A. (2012). An inventory of peroxisomal proteins and pathways in Drosophila melanogaster. Traffic **13**: 1378–1392.

Fodor, K., Wolf, J., Erdmann, R., Schliebs, W., and Wilmanns, M. (2012). Molecular requirements for peroxisomal targeting of alanine-glyoxylate aminotransferase as an essential determinant in primary hyperoxaluria type 1. PLoS Biol. **10**: e1001309.

Freitas, M.O., Francisco, T., Rodrigues, T. a, Alencastre, I.S., Pinto, M.P., Grou, C.P., Carvalho, A.F., Fransen, M., Sá-Miranda, C., and Azevedo, J.E. (2011). PEX5 protein binds monomeric catalase blocking its tetramerization and releases it upon binding the N-terminal domain of PEX14. J. Biol. Chem. **286**: 40509–19.

Fujiki, Y., Yagita, Y., and Matsuzaki, T. (2012). Peroxisome biogenesis disorders: molecular basis for impaired peroxisomal membrane assembly: in metabolic functions and biogenesis of peroxisomes in health and disease. Biochim. Biophys. Acta **1822**: 1337–42.

Fulda, M., Shockey, J., Werber, M., Wolter, F.P., and Heinz, E. (2002). Two long-chain acyl-CoA synthetases from Arabidopsis thaliana involved in peroxisomal fatty acid beta-oxidation. Plant J. **32**: 93–103.

Galland, N., de Walque, S., Voncken, F.G.J., Verlinde, C.L.M.J., and Michels, P. a M. (2010). An internal sequence targets Trypanosoma brucei triosephosphate isomerase to glycosomes. Mol. Biochem. Parasitol. **171**: 45–9.

Goto, S., Mano, S., Nakamori, C., and Nishimura, M. (2011). Arabidopsis ABERRANT PEROXISOME MORPHOLOGY9 is a peroxin that recruits the PEX1-PEX6 complex to peroxisomes. Plant Cell **23**: 1573–87.

Grimm, M.O.W., Kuchenbecker, J., Rothhaar, T.L., Grösgen, S., Hundsdörfer, B., Burg, V.K., Friess, P., Müller, U., Grimm, H.S., Riemenschneider, M., and Hartmann, T. (2011). Plasmalogen synthesis is regulated via alkyl-dihydroxyacetonephosphate-synthase by amyloid precursor protein processing and is affected in Alzheimer's disease. J. Neurochem. **116**: 916–25.

Grou, C.P., Carvalho, a F., Pinto, M.P., Alencastre, I.S., Rodrigues, T. a, Freitas, M.O., Francisco, T., Sá-Miranda, C., and Azevedo, J.E. (2009a). The peroxisomal protein import machinery--a case report of transient ubiquitination with a new flavor. Cell. Mol. Life Sci. **66**: 254–62.

Grou, C.P., Carvalho, A.F., Pinto, M.P., Huybrechts, S.J., Sá-Miranda, C., Fransen, M., and Azevedo, J.E. (2009b). Properties of the ubiquitin-pex5p thiol ester conjugate. J. Biol. Chem. **284**: 10504–13.

Grou, C.P., Carvalho, A.F., Pinto, M.P., Wiese, S., Piechura, H., Meyer, H.E., Warscheid, B., Sá-Miranda, C., and Azevedo, J.E. (2008). Members of the E2D (UbcH5) family mediate the ubiquitination of the conserved cysteine of Pex5p, the peroxisomal import receptor. J. Biol. Chem. **283**: 14190–7.

Grunau, S., Schliebs, W., Linnepe, R., Neufeld, C., Cizmowski, C., Reinartz, B., Meyer, H.E., Warscheid, B., Girzalsky, W., and Erdmann, R. (2009). Peroxisomal Targeting of PTS2 Pre-Import Complexes in the Yeast Saccharomyces cerevisiae. Traffic **10**: 451–460.

Gunkel, K., Dijk, R. Van, Veenhuis, M., Klei, I.J. Van Der, and Lara, A.- (2004). Routing of Hansenula polymorpha Alcohol Oxidase : An Alternative Peroxisomal Protein-sorting Machinery Name. Mol. Biol. Cell **15**: 1347–1355.

Hasan, S., Platta, H.W., and Erdmann, R. (2013). Import of proteins into the peroxisomal matrix. Front. Physiol. **4**: 261.

He, Y. and Gan, S. (2002). A Gene Encoding an Acyl Hydrolase Is Involved in Leaf Senescence in Arabidopsis. Plant Cell **14**: 805–815.

Helm, M., Lück, C., Prestele, J., Hierl, G., Huesgen, P.F., Fröhlich, T., Arnold, G.J., Adamska, I., Görg, A., Lottspeich, F., and Gietl, C. (2007). Dual specificities of the glyoxysomal/peroxisomal processing protease Deg15 in higher plants. Proc. Natl. Acad. Sci. U. S. A. **104**: 11501–6.

Heo, J.-M. and Rutter, J. (2011). Ubiquitin-dependent mitochondrial protein degradation. Int. J. Biochem. Cell Biol. **43**: 1422–6.

Hu, J., Aguirre, M., Peto, C., Alonso, J., Ecker, J., and Chory, J. (2002). A role for peroxisomes in photomorphogenesis and development of Arabidopsis. Science **297**: 405–9.

Hu, J., Baker, A., Bartel, B., Linka, N., Mullen, R.T., Reumann, S., and Zolman, B.K. (2012). Plant peroxisomes: biogenesis and function. Plant Cell **24**: 2279–303.

Huhse, B., Rehling, P., Albertini, M., Blank, L., Meller, K., and Kunau, W. (1998). Pex17p of Saccharomyces cerevisiae Is a Novel Peroxin and Component of the Peroxisomal Protein Translocation Machinery. J. Cell Biol. **140**: 49–60.

Islinger, M., Li, K.W., Seitz, J., Völkl, A., and Lüers, G.H. (2009). Hitchhiking of Cu/Zn superoxide dismutase to peroxisomes--evidence for a natural piggyback import mechanism in mammals. Traffic **10**: 1711–21.

Jung, S., Marelli, M., Rachubinski, R. a, Goodlett, D.R., and Aitchison, J.D. (2010). Dynamic changes in the subcellular distribution of Gpd1p in response to cell stress. J. Biol. Chem. **285**: 6739–49.

Karnik, S.K. and Trelease, R.N. (2005). Arabidopsis Peroxin 16 Coexists at Steady State in Peroxisomes and Endoplasmic Reticulum 1. Plant Physiol. **138**: 1967–1981.

Kaur, N. and Hu, J. (2009). Dynamics of peroxisome abundance: a tale of division and proliferation. Curr. Opin. Plant Biol. **12**: 781–8.

Kaur, N., Zhao, Q., Xie, Q., and Hu, J. (2013). Arabidopsis RING peroxins are E3 ubiquitin ligases that interact with two homologous ubiquitin receptor proteins(F). J. Integr. Plant Biol. **55**: 108–20.

Kiel, J. a K.W., Veenhuis, M., and van der Klei, I.J. (2006). PEX genes in fungal genomes: common, rare or redundant. Traffic **7**: 1291–303.

Kiel, J. a. K.W., Emmrich, K., Meyer, H.E., and Kunau, W.-H. (2004). Ubiquitination of the Peroxisomal Targeting Signal Type 1 Receptor, Pex5p, Suggests the Presence of a Quality Control Mechanism during Peroxisomal Matrix Protein Import. J. Biol. Chem. **280**: 1921–1930.

Klein, A.T.J., van den Berg, M., Bottger, G., Tabak, H.F., and Distel, B. (2002). Saccharomyces cerevisiae acyl-CoA oxidase follows a novel, non-PTS1, import pathway into peroxisomes that is dependent on Pex5p. J. Biol. Chem. **277**: 25011–9.

Koo, A.J.K., Chung, H.S., Kobayashi, Y., and Howe, G. a (2006). Identification of a peroxisomal acyl-activating enzyme involved in the biosynthesis of jasmonic acid in Arabidopsis. J. Biol. Chem. **281**: 33511–20.

Kragt, A., Voorn-Brouwer, T., van den Berg, M., and Distel, B. (2005). The Saccharomyces cerevisiae peroxisomal import receptor Pex5p is monoubiquitinated in wild type cells. J. Biol. Chem. **280**: 7867–74.

Kunze, M., Pracharoenwattana, I., Smith, S.M., and Hartig, A. (2006). A central role for the peroxisomal membrane in glyoxylate cycle function. Biochim. Biophys. Acta **1763**: 1441–52.

Kurochkin, I. V, Mizuno, Y., Konagaya, A., Sakaki, Y., Schönbach, C., and Okazaki, Y. (2007). Novel peroxisomal protease Tysnd1 processes PTS1- and PTS2-containing enzymes involved in beta-oxidation of fatty acids. EMBO J. **26**: 835–45.

Lasorsa, F.M., Pinton, P., Palmieri, L., Scarcia, P., Rottensteiner, H., Rizzuto, R., and Palmieri, F. (2008). Peroxisomes as novel players in cell calcium homeostasis. J. Biol. Chem. **283**: 15300–8.

Lazarow, P.B. (2006). The import receptor Pex7p and the PTS2 targeting sequence. Biochim. Biophys. Acta **1763**: 1599–604.

Lee, P.R. and Raymond, G. V (2013). Child neurology: Zellweger syndrome. Neurology **80**: e207–10.

Léon, S., Goodman, J.M., and Subramani, S. (2006a). Uniqueness of the mechanism of protein import into the peroxisome matrix: transport of folded, co-factor-bound and oligomeric proteins by shuttling receptors. Biochim. Biophys. Acta **1763**: 1552–64.

Léon, S., Zhang, L., McDonald, W.H., Yates, J., Cregg, J.M., and Subramani, S. (2006b). Dynamics of the peroxisomal import cycle of PpPex20p: ubiquitin-dependent localization and regulation. J. Cell Biol. **172**: 67–78.

Lingard, M.J. and Bartel, B. (2009). Arabidopsis LON2 is necessary for peroxisomal function and sustained matrix protein import. Plant Physiol. **151**: 1354–65.

Lingner, T., Kataya, A.R., Antonicelli, G.E., Benichou, A., Nilssen, K., Chen, X.-Y., Siemsen, T., Morgenstern, B., Meinicke, P., and Reumann, S. (2011). Identification of novel plant peroxisomal targeting signals by a combination of machine learning methods and in vivo subcellular targeting analyses. Plant Cell **23**: 1556–72.

Linka, N., Theodoulou, F.L., Haslam, R.P., Linka, M., Napier, J. a, Neuhaus, H.E., and Weber, A.P.M. (2008). Peroxisomal ATP import is essential for seedling development in Arabidopsis thaliana. Plant Cell **20**: 3241–57.

Liu, X. and Subramani, S. (2013). Unique requirements for mono- and polyubiquitination of the peroxisomal targeting signal co-receptor, Pex20. J. Biol. Chem. **288**: 7230–40.

Ludwig-muller, J., Epstein, E., Institut, B., and Main, F. (1994). Indole-3-butyric acid in Arabidopsis thaliana III . In vivo biosynthesis. Plant Growth Regul. **14**: 7–14.

Ma, C., Hagstrom, D., Polley, S.G., and Subramani, S. (2013). Redox-regulated cargo binding and release by the peroxisomal targeting signal receptor, Pex5. J. Biol. Chem. **288**: 27220–31.

Matsumoto, N., Tamura, S., and Fujiki, Y. (2003). The pathogenic peroxin Pex26p recruits the Pex1p-Pex6p AAA ATPase complexes to peroxisomes. Nat. Cell Biol. **5**: 454–60.

Maurino, V.G. and Peterhansel, C. (2010). Photorespiration: current status and approaches for metabolic engineering. Curr. Opin. Plant Biol. **13**: 249–56.

Meijer, W.H., Gidijala, L., Fekken, S., Kiel, J. a K.W., van den Berg, M. a, Lascaris, R., Bovenberg, R. a L., and van der Klei, I.J. (2010). Peroxisomes are required for efficient penicillin biosynthesis in Penicillium chrysogenum. Appl. Environ. Microbiol. **76**: 5702–9.

Meinecke, M., Cizmowski, C., Schliebs, W., Krüger, V., Beck, S., Wagner, R., and Erdmann, R. (2010). The peroxisomal importomer constitutes a large and highly dynamic pore. Nat. Cell Biol. **12**: 273–7.

Moroney, J. V, Jungnick, N., Dimario, R.J., and Longstreth, D.J. (2013). Photorespiration and carbon concentrating mechanisms: two adaptations to high O2, low CO2 conditions. Photosynth. Res. **117**: 121–31.

Motley, A.M., Hettema, E.H., Ketting, R., Plasterk, R., and Tabak, H.F. (2000). Caenorhabditis elegans has a single pathway to target matrix proteins to peroxisomes. Eur. Mol. Biol. Organ. **1**: 40–46.

Niederhoff, K., Meindl-Beinker, N.M., Kerssen, D., Perband, U., Schäfer, A., Schliebs, W., and Kunau, W.-H. (2005). Yeast Pex14p possesses two functionally distinct Pex5p and one Pex7p binding sites. J. Biol. Chem. **280**: 35571–8.

Nishimura, M., Yamaguchi, J., Mori, H., Akazawa, T., and Yokota, S. (1986). Immunocytochemical Directly Greening. Plant Physiol. **80**: 313–316.

Nito, K., Kamigaki, A., Kondo, M., Hayashi, M., and Nishimura, M. (2007). Functional classification of Arabidopsis peroxisome biogenesis factors proposed from analyses of knockdown mutants. Plant Cell Physiol. **48**: 763–74.

Novikoff, a. B., Novikoff, P.M., Davis, C., and Quintana, N. (1973). Studies on Microperoxisomes V. Are Microperoxisomes Ubiquitous in Mammalian Cells? J. Histochem. Cytochem. **21**: 737–755.

Okumoto, K., Kametani, Y., and Fujiki, Y. (2011a). Two proteases, trypsin domain-containing 1 (Tysnd1) and peroxisomal lon protease (PsLon), cooperatively regulate fatty acid β-oxidation in peroxisomal matrix. J. Biol. Chem. **286**: 44367–79.

Okumoto, K., Misono, S., Miyata, N., Matsumoto, Y., Mukai, S., and Fujiki, Y. (2011b). Cysteine ubiquitination of PTS1 receptor Pex5p regulates Pex5p recycling. Traffic **12**: 1067–83.

Oshima, Y., Kamigaki, A., Nakamori, C., Mano, S., Hayashi, M., Nishimura, M., and Esaka, M. (2008). Plant catalase is imported into peroxisomes by Pex5p but is distinct from typical PTS1 import. Plant Cell Physiol. **49**: 671–7.

Perlmutter, D.H. (2006). Pathogenesis of chronic liver injury and hepatocellular carcinoma in alpha-1-antitrypsin deficiency. Pediatr. Res. **60**: 233–8.

Petriv, O.I., Tang, L., Titorenko, V.I., and Rachubinski, R. a (2004). A new definition for the consensus sequence of the peroxisome targeting signal type 2. J. Mol. Biol. **341**: 119–34.

Pires, J.R., Hong, X., Brockmann, C., Volkmer-Engert, R., Schneider-Mergener, J., Oschkinat, H., and Erdmann, R. (2003). The ScPex13p SH3 Domain Exposes Two Distinct Binding Sites for Pex5p and Pex14p. J. Mol. Biol. **326**: 1427–1435.

Platta, H.W. and Erdmann, R. (2007). Peroxisomal dynamics. Trends Cell Biol. **17**: 474–84.

Platta, H.W., Grunau, S., Rosenkranz, K., Girzalsky, W., and Erdmann, R. (2005). Functional role of the AAA peroxins in dislocation of the cycling PTS1 receptor back to the cytosol. Nat. Cell Biol. **7**: 817–22.

Platta, H.W., Hagen, S., Reidick, C., and Erdmann, R. (2014). The peroxisomal receptor dislocation pathway: to the exportomer and beyond. Biochimie **98**: 16–28.

Pracharoenwattana, I. and Smith, S.M. (2008). When is a peroxisome not a peroxisome? Trends Plant Sci. **13**: 522–5.

Quan, S., Yang, P., Cassin-Ross, G., Kaur, N., Switzenberg, R., Aung, K., Li, J., and Hu, J. (2013). Proteome analysis of peroxisomes from etiolated Arabidopsis seedlings identifies a peroxisomal protease involved in β-oxidation and development. Plant Physiol. **163**: 1518–38.

Radhika, V., Kost, C., Boland, W., and Heil, M. (2010). The Role of Jasmonates in Floral Nectar Secretion. PLoS One **5**: e9265.

Reumann, S., Ma, C., Lemke, S., and Babujee, L. (2004). AraPerox . A Database of Putative Arabidopsis Proteins. Plant Physiol. **136**: 2587–2608.

Reumann, S., Quan, S., Aung, K., Yang, P., Manandhar-Shrestha, K., Holbrook, D., Linka, N., Switzenberg, R., Wilkerson, C.G., Weber, A.P.M., Olsen, L.J., and Hu, J. (2009). In-depth proteome analysis of Arabidopsis leaf peroxisomes combined

with in vivo subcellular targeting verification indicates novel metabolic and regulatory functions of peroxisomes. Plant Physiol. **150**: 125–43.

Rucktäschel, R., Girzalsky, W., and Erdmann, R. (2011). Protein import machineries of peroxisomes. Biochim. Biophys. Acta **1808**: 892–900.

Rylott, E.L., Eastmond, P.J., Gilday, A.D., Slocombe, S.P., Larson, T.R., Baker, A., and Graham, I. a (2006). The Arabidopsis thaliana multifunctional protein gene (MFP2) of peroxisomal beta-oxidation is essential for seedling establishment. Plant J. **45**: 930–41.

Sautter, C. (1986). Microbody transition in greening watermelon cotyledons Double immunocytochemical labeling of isocitrate lyase and hydroxypyruvate reductase. Planta **167**: 491–503.

Schell-steven, A., Stein, K., Amoros, M., Landgraf, C., Volkmer-engert, R., Erdmann, R., and Rottensteiner, H. (2005). Identification of a Novel , Intraperoxisomal Pex14-Binding Site in Pex13 : Association of Pex13 with the Docking Complex Is Essential for Peroxisomal Matrix Protein Import Identification of a Novel , Intraperoxisomal Pex14-Binding Site in Pex13 : Associat. Mol. Cell. Biol. **25**: 3007–3018.

Schilmiller, A.L., Koo, A.J.K., and Howe, G. a (2007). Functional diversification of acyl-coenzyme A oxidases in jasmonic acid biosynthesis and action. Plant Physiol. **143**: 812–24.

Schliebs, W. and Kunau, W.-H. (2006). PTS2 co-receptors: diverse proteins with common features. Biochim. Biophys. Acta **1763**: 1605–12.

Schuhmann, H., Huesgen, P.F., Gietl, C., and Adamska, I. (2008). The DEG15 serine protease cleaves peroxisomal targeting signal 2-containing proteins in Arabidopsis. Plant Physiol. **148**: 1847–56.

Schumann, U., Wanner, G., Veenhuis, M., Schmid, M., and Gietl, C. (2003). AthPEX10, a nuclear gene essential for peroxisome and storage organelle formation during Arabidopsis embryogenesis. Proc. Natl. Acad. Sci. U. S. A. **100**: 9626–31.

Shiozawa, K., Konarev, P. V, Neufeld, C., Wilmanns, M., and Svergun, D.I. (2009). Solution structure of human Pex5.Pex14.PTS1 protein complexes obtained by small angle X-ray scattering. J. Biol. Chem. **284**: 25334–42.

Shockey, J.M., Fulda, M.S., and Browse, J.A. (2002). Arabidopsis Contains Nine Long-Chain Acyl-Coenzyme A Synthetase Genes That Participate in Fatty Acid and Glycerolipid Metabolism 1. Plant Physiol. **129**: 1710–1722.

Sibirny, A.A. (2012). Molecular mechanisms of peroxisome biogenesis in yeasts. Mol. Biol. **46**: 11–26.

Sparkes, I.A., Brandizzi, F., Slocombe, S.P., El-shami, M., Hawes, C., and Baker, A. (2003). An Arabidopsis pex10 Null Mutant Is Embryo Lethal , Implicating Peroxisomes in an Essential Role during. Plant Physiol. **133**: 1809–1819.

Stanley, W. a, Filipp, F. V, Kursula, P., Schüller, N., Erdmann, R., Schliebs, W., Sattler, M., and Wilmanns, M. (2006). Recognition of a functional peroxisome type 1 target by the dynamic import receptor pex5p. Mol. Cell **24**: 653–63.

Stein, K., Schell-steven, A., Erdmann, R., and Rottensteiner, H. (2002). Interactions of Pex7p and Pex18p / Pex21p with the Peroxisomal Docking Machinery : Implications for the First Steps in PTS2 Protein Import Interactions of Pex7p and Pex18p / Pex21p with the Peroxisomal Docking Machinery : Implications for the First Steps. Mol. Cell. Biol. **22**: 6056–6069.

Titus, D.E. and Becker, W.M. (1985). Investigation of the glyoxysome-peroxisome transition in germinating cucumber cotyledons using double-label immunoelectron microscopy. J. Cell Biol. **101**: 1288–99.

Troncoso-Ponce, M. a, Cao, X., Yang, Z., and Ohlrogge, J.B. (2013). Lipid turnover during senescence. Plant Sci. **205-206**: 13–9.

Vrebalov, J., Giovannoni, J.J., Yagi, K., Kobayashi, Y., and Howe, G.A. (2005). Role of b -Oxidation in Jasmonate Biosynthesis and Systemic Wound Signaling in Tomato. Plant Cell **17**: 971–986.

Walton, P.A. (1996). Import of Stably-folded Proteins into Peroxisomes. Ann. N. Y. Acad. Sci. **804**: 76–85.

Wang, D., Visser, N. V, Veenhuis, M., and van der Klei, I.J. (2003). Physical interactions of the peroxisomal targeting signal 1 receptor pex5p, studied by fluorescence correlation spectroscopy. J. Biol. Chem. **278**: 43340–5.

Widhalm, J.R., Ducluzeau, A.-L., Buller, N.E., Elowsky, C.G., Olsen, L.J., and Basset, G.J.C. (2012). Phylloquinone (vitamin K(1)) biosynthesis in plants: two peroxisomal thioesterases of lactobacillales origin hydrolyze 1,4-dihydroxy-2-naphthoyl-coa. Plant J. **71**: 205–15.

Williams, C. (2014). Going against the flow: a case for peroxisomal protein export. Biochim. Biophys. Acta **1843**: 1386–92.

Williams, C. and Distel, B. (2006). Pex13p: docking or cargo handling protein? Biochim. Biophys. Acta **1763**: 1585–91.

Yamaguchi, K., Mori, H., and Nishimura, M. (1995). A novel isoenzyme of ascorbate peroxidase localized on glyoxysomal and leaf peroxisomal membranes in pumpkin. Plant Cell Physiol. **36**: 1157–62.

Yang, X., Purdue, P.E., and Lazarow, P.B. (2001). Eci1p uses a PTS1 to enter peroxisomes: either its own or that of a partner, Dci1p. Eur. J. Cell Biol. **80**: 126–38.

Yang, Z. and Ohlrogge, J.B. (2009). Turnover of fatty acids during natural senescence of Arabidopsis, Brachypodium, and switchgrass and in Arabidopsis beta-oxidation mutants. Plant Physiol. **150**: 1981–9.

Zolman, B.K. and Bartel, B. (2004). An Arabidopsis indole-3-butyric acid-response mutant defective in PEROXIN6, an apparent ATPase implicated in peroxisomal function. Proc. Natl. Acad. Sci. U. S. A. **101**: 1786–91.

Zolman, B.K., Monroe-Augustus, M., Thompson, B., Hawes, J.W., Krukenberg, K. a, Matsuda, S.P., and Bartel, B. (2001). chy1, an Arabidopsis mutant with impaired beta-oxidation, is defective in a peroxisomal beta-hydroxyisobutyryl-CoA hydrolase. J. Biol. Chem. **276**: 31037–46.

Zolman, B.K., Yoder, a, and Bartel, B. (2000). Genetic analysis of indole-3-butyric acid responses in Arabidopsis thaliana reveals four mutant classes. Genetics **156**: 1323–37.

CHAPTER 2

Characterization of the *Arabidopsis* peroxisomal protein UBIQUITIN-CONJUGATING ENZYME 22

This project was initiated by Dr. Navneet Kaur. Confocal microscopy images (Figure 2.4A) were obtained by Dr. Navneet Kaur.

Fatty acid composition analysis data (Figure 2.13 C&D) was obtained by Dr. Weili Yang.

Abstract

Peroxisomes are multifunctional eukaryotic organelles that mediate a broad range of metabolic and biochemical processes critical for growth and development. Many proteins involved in peroxisome matrix protein import, such as PEX5, PEX7 and PEX14, have been identified. However, our knowledge of the mechanism behind matrix protein export and degradation processes is still scarce. Here I characterized a novel member of the peroxisomal ubiquitin-proteasome system, *Arabidopsis* ubiquitin-conjugating enzyme 22 (AtUBC22). I demonstrated that YFP-UBC22 localizes to peroxisomes, and this localization relies on a tripeptide KRL> located at the C-terminus of UBC22. Null *ubc22* mutants have longer primary roots and larger leaves at early developmental stages, are hypersensitive to exogenous IBA, and yield larger seeds despite of having reduced fertility. In summary, *Arabidopsis* UBC22 is a peroxisomal protein involved in IBA metabolism and participating in plant growth and reproduction.

2.1 Introduction

Peroxisomes are critical organelles that are present in most eukaryotes, housing a broad range of metabolic and biochemical processes that are vital for cells and organisms in many aspects. Defects in peroxisomes have been linked to several severe developmental disorders and fatal human diseases, highlighting the importance of peroxisomes in maintaining normal cellular functions. Fatty acid β-oxidation and hydrogen peroxide (H_2O2) detoxification are peroxisomal functions well conserved from yeast to man. Proteomic analyses of peroxisomes have identified about 85 peroxisomal genes in *Homo sapiens* (human) and 61 genes in *Saccharomyces cerevisiae* (Schrader and Fahimi, 2008). Surprisingly, around 137 peroxisomal genes have been identified in *Arabidopsis thaliana* (http://www.peroxisome.msu.edu/), indicating that compared with yeast and human, plant peroxisomes may bear more pathways and functions than we once thought.

In eukaryotes, organisms employ post-translational modifications (PTMs) to increase the functional diversity of the proteome and dynamically coordinate signaling networks. PTMs influence cells in almost all aspects through regulating protein activities, localization, degradation, and protein interaction with other proteins, nucleic acids, lipids, and cofactors. PTMs involve phosphorylation, ubiquitination, methylation, acetylation, *etc.* Among these mechanisms, the ubiquitin (Ub)-proteasome system (UPS) is utilized by cells to regulate the degradation of intracellular proteins and as a type of 'quality control' (Varshavsky, 2012). Modification of protein by ubiquitination also contributes to cell-cycle control, stress response, DNA repair, growth-factor signaling, transcription, gene silencing, and other cellular processes (Hurley *et al.*, 2006).

In order to destroy and recycle misfolded proteins or maintain proteinexpression at certain levels, UPS modifies its substrates by attaching a polyubiquitin chain to it, so that the substrate can be recognized by the 26s proteasome and be degraded. UPS can also perform mono-ubiquitination to regulate protein activity, for instance histone H2B mono-ubiquitination is involved in transcription regulation, differentiation as well as DNA repair (Bonnet *et al.*, 2014). In *Arabidopsis*, around 6% of the genome is dedicated to the UPS (Hua and Vierstra, 2011).

The ubiquitination system consists of ubiquitin-activating enzymes (E1), ubiquitin-conjugating enzymes (E2), and ubiquitin ligases (E3), which act sequentially in the substrate ubiquitination reaction. Ub is a 8.5-kDa polypeptide consisting of 76 amino acids and present in nearly all eukaryotic organisms. The initial step of this reaction is the ATP-dependent activation of ubiquitin (Ub), in which the last residue of Ub (Gly76) is attached to a Cys residue on the E1 enzyme via a thioester bond (Varshavsky, 2012). E1 then transfers the “activated” Ub moiety to the active site Cys of an E2 enzyme through a trans (thio) esterification reaction. At the final step of the ubiquitination cascade, E2 together with the “activated” Ub moiety bind to an E3 enzyme and form E2-E3 Ub ligase holoenzymes. E3 functions as the target protein recognition module that is able to interact with both E2 and the specific substrate at the same time. After the E2-E3 Ub ligase holoenzyme recognizes the target protein, E2 passes the Ub moiety to the Lys residue of the target protein via an isopeptide bond between the C-terminal Gly of the Ub moiety and a Lys on the substrate. Substrates are able to attach polyubiquitin chains through the catalyzation of E2. Ubiquitination can lead to diverse effects on the target protein depending on the position of the Lys residue that the Ub moiety is bonded

with, and the number and topology of the mono-ubiquitin or ubiquitin chains added to the substrate. In eukaryotes, an E1 is able to bind to a dozen E2s, which can then bind to hundreds of E3s. While E3s control substrate selection, E2s are involved in the selection of the Lys residue to attach the ubiquitin chain to, thereby deciding the cellular fate of the substrate (van Wijk and Timmers, 2010). In order to bind to Ub, a specific domain, UBDs, which is required by enzymes that catalyze ubiquitylation or deubiquitylation. UBDs are a class of ubiquitin-binding domains that non-covalently bind to ubiquitin (Hicke *et al.*, 2005). Currently there are at least 20 known UBD domains: UBA, UIM, MIU, DUIM, CUE, GAT, VHS, NZF, A20 ZnF, UBP ZnF, PRU, UBZ, UEV, UBCc, UBM, UBAN, GLUE, SH3, Jab1/MPN and PFU (Dikic *et al.*, 2009; Hurley *et al.*, 2006).

At present, several UPS components have been identified to be involved in peroxisome related pathways. In plants and yeasts, the peroxisomal matrix protein receptor PEX5 is dislocated from the peroxisome matrix after delivering cargo proteins, and moves back to the cytosol for either recycling or degradation in an ubiquitin-dependent manner. In yeast, and probably also in plants, this process is mediated by the RING-finger complex (Pex2p, Pex10p and Pex12p) that displays ubiquitin-protein ligase (E3) activity, the ubiquitin-conjugating enzyme (E2) Pex4p/ScUBC21 together with its membrane anchor protein Pex22p, and two AAA ATPase family members Pex1p and Pex6p (Hasan *et al.*, 2013). Ubiquitination of Pex5p provides the export signal for Pex5p, allowing it to be recognized by the dislocation machinery (Okumoto et al., 2011). Pex5p depends on the RING protein Pex12p (E3) and Pex4p (E2) for mono-ubiquitination, after which it is dislocated to the cytosol via Pex1p and Pex6p (Grou et

al., 2009). In mammals, HsUBC E2D1/2/3 (UbcH5A/B/C) (E2) might be the functional counterparts of the yeast Pex4p, as it catalyzes the mono-ubiquitination of PEX5 (Grou et al., 2008).

Little is known about the function of the plant peroxisomal associated UPS. Although plant peroxisomal RING proteins PEX2, PEX10 and PEX10 possess E3 Ub ligase activity, their substrates have not been identified. The biochemical function of plant PEX4 has not been demonstrated, either. It is also unknown whether there are other components of the peroxisomal UPS in plants. To better understand how plant peroxisomal function is regulated by the UPS and to identify additional components of this system, I identified and characterized a peroxisomal localized ubiquitin-conjugating enzyme, AtUBC22, in *Arabidopsis*. Through cell biological and genetic analyses, I confirmed the peroxisomal localization of AtUBC22 and showed that it is involved in peroxisomal IBA metabolism and plant growth and reproduction.

2.2 RESULTS

2.2.1 AtUBC22 is an E2 enzyme predicted to be peroxisomal

In order to identify additional proteins involved in the *Arabidopsis* peroxisome protein proteolytic processes, we employed two criteria to search The *Arabidopsis* Information Resource (TAIR) database (TAIR: https://www.arabidopsis.org/ (Garcia-Hernandez *et al.*, 2002)). First, we searched for proteins that contain a putative ubiquitin-conjugating catalytic (UBCc) domain by consulting the TAIR Protein Domain

database (ftp://ftp.arabidopsis.org/home/tair/Proteins/Domains/TAIR10_all.domains). Several previously identified peroxisome-related ubiquitin (Ub)-proteasome system (UPS) members share this trait in diverse species, i.e. yeast Pex4p (UBC10, PAS2), *Arabidopsis* PEX4 (UBC21) and human E2D1/2/3 (UbcH5A/B/C). I identified a total of 49 *Arabidopsis* proteins that contain UBCc domain (Table 2.1).

Second, I searched the 49 candidates for putative peroxisome targeting signals (PTSs), using a published database and protein targeting prediction website TargetP (http://www.cbs.dtu.dk/services/TargetP/) (database available at http://www.plantcell.org/content/23/4/1556.full, (Lingner *et al.*, 2011)). As a result, I was able to narrow to a single gene, At5g05080, which encodes ubiquitin-conjugating enzyme 22 (UBC22). UBC22 contains an UBCc domain with a conserved active-site Cys residue as well as an experimentally verified C-terminal PTS1 tripeptide KRL>.

Previous *in vitro* ubiquitination assays reported that UBC22 has E3-independent activity, implying that UBC22 is able to catalyze the formation of a poly-ubiquitin chain *in vitro* without the presence of an E3 ligase. Converting the conserved active-site Cys residue to alanine (Ala) resulted in the disability of UBC22 to bind to ubiquitin, thus indicating that this conserved Cys is necessary to maintain the basic function of UBC22 (Takahashi *et al.*, 2009; Kraft *et al.*, 2005). Although UBC22 was experimentally verified to be able to catalyze the formation of the poly-ubiquitin chain without E3, whether this activity also occurs *in vivo* in *Arabidopsis* and its regulatory function is unknown. Several UBC proteins that possess E3-independent activity have been reported in other species. For example, yeast Cdc34p is believed to regulate its own levels (Skowyra *et al.*, 1999). In addition, unlike most Arabidopsis UBC proteins that share higher

similarities with other Arabidopsis UBC proteins, UBC22 displays high sequence similarity to a human UBC protein HsUBE2S/EPF5, which has a higher expression level in cancer tissues compared with normal tissues (Kraft *et al.*, 2005; Welsh *et al.*, 2001)

To further characterize UBC22. I asked the following questions: Is UBC22 a peroxisome-localized protein? What is the possible physiological role(s) of AtUBC22 in plants and which peroxisomal metabolic pathway is it involved in? What are its possible substrates in plants?

2.2.2 UBC22 amino acid sequence analysis

The *UBC22* gene has five exons (Figure 2.1A). Its protein product contains a previously verified UBCc domain near the N-terminus that harbors a conserved catalytic Cys residue required for UBC22 activity (Kraft *et al.*, 2005; Takahashi *et al.*, 2009), and a non-canonical PTS1 tripeptide KRL> at its C-terminus (Figure 2.1B). Protein topology analysis of UBC22 amino acids sequence predicted by TMHMM Server v. 2.0 (http://www.cbs.dtu.dk/services/TMHMM/ (Krogh *et al.*, 2001)) and plant membrane protein database (Aramemnon: http://aramemnon.botanik.uni-koeln.de/ (Schwacke *et al.*, 2003)) showed that UBC22 does not contain a hydrophobic region that may constitue a transmembrane domain, indicating that AtUBC22 may not be an integral membrane protein.

Phylogenetic analysis showed that within all known UBCs in *Arabidopsis* and the yeast *S. cerevisia,* AtUBC22 has the highest sequence similarity to yeast

ScUbc10/Pex4p and *Arabidopsis* PEX4 (Figure 2.2). Amino acid sequence alignment of AtUBC22 and selected known peroxisomal related E2s showed that AtUBC22 shares 35%, 41% and 36% amino acid identities with HsUBC E2D1/2/3 (UbcH5A/B/C), ScUbc10/Pex4p and AtUBC21/PEX4, respectively. Further amino acid sequence analysis of AtUBC22 using ClustalW2 predicted that Cys94 is the conserved E2 active Cys residue in AtUBC22 (ClustalW2: http://www.ebi.ac.uk/Tools/msa/clustalw2/) (Figure 2.3).

2.2.3 AtUBC22 is localized to *Arabidopsis* peroxisomes and its C-terminal tripeptide KRL> is required for proper peroxisome targeting

In order to confirm the predicted localization of UBC22, we co-expressed in *Arabidopsis* a peroxisome marker DsRed-PTS1, and the $35S_{pro}$: Green Fluorescent Protein (GFP)-UBC22 fusion protein. Subcellular localization of GFP-UBC22 was examined using confocal laser scanning microscopy in *Arabidopsis* T1 plants by Dr. Navneet Kaur. As shown in Figure 2.4A, GFP-UBC22 was co-localized with fluorescence spots labeled by the peroxisome marker DsRed-PTS1, few GFP-UBC22 signal were observed in the cytosol (Figure 2.4A). However, GFP-UBC22 signals were largely lost in T2 plants (data not shown). To confirm the localization of AtUBC22, I generated a *$35S_{pro}$: Yellow Fluorescent Protein (YFP)-UBC22* (full length *UBC22* CDS) fusion construct and transformed it into *Arabidopsis.* T1 transgenic seedlings are being screened as this thesis is written. I also transiently co-expressed *$35S_{pro}$: YFP-UBC22* with the peroxisomal marker DsRed-PTS1 in *Nicotiana tabacum* (Tobacco).

Fluorescence microscopy of the infiltrated tobacco leaf epidermal cells showed that, like GFP-UBC22, which was shown to be localized to the peroxisome in *Arabidopsis*, YFP-UBC22 also co-localized with DsRed-PTS1 in tobacco.

To determine whether the tripeptide KRL> (Lys-Arg-Leu) at the very C-terminal end of UBC22 is required for AtUBC22's peroxisomal targeting, I tested the localization of YFP-UBC22ΔKRL, in which KRL> was deleted. Fluorescence microscopy of tobacco leaf epidermal cells showed that the fusion proteins are localized to the cytosol instead of peroxisomes (Figure 2.4B).

The above data indicate that AtUBC22 is localized to peroxisomes, and the C-terminal tripeptide KRL> is required for the proper targeting of AtUBC22 to peroxisomes.

2.2.4 *UBC22* is ubiquitously expressed in plants

To investigate the expression pattern of *UBC22* in *Arabidopsis*, we searched GENEVESTIGATOR database (https://www.genevestigator.com/gv/plant.jsp) for information obtained from microarray-based analyses (Hruz *et al.*, 2008). This resource uses publicly available microarray data to generate expression profiling of genes. *UBC22* is highly expressed in nearly all *Arabidopsis* tissues throughout the life-time of a plant (Figure 2.5 A). Further tissue specific expression profiling shows that *UBC22* has very high levels of expression in pollen and pistil (Figure 2.5B).

2.4.5 Null mutants of *UBC22* are more sensitive to exogenous IBA

To examine the possible roles of UBC22 in peroxisome function, I characterized two *UBC22* T-DNA insertion alleles: *ubc22-1* (GK-642C08) and *ubc22-2* (SALK_011800) (Figure 2.1A) (Kleinboelting *et al.*, 2012). Both lines are in Col-0 background and have T-DNA insertion in the fifth exon - the last exon of *UBC22* (Figure 2.1A). I conducted reverse transcription PCR (RT-PCR) to analyze the transcript levels of *UBC22* in *ubc22-1* and *ubc22-2.* Both alleles are null mutant lines, as full-length? *UBC22* transcripts were not detected in either allele (Figure 2.6).

Physiological assays were performed on the null *ubc22* mutants to determine if AtUBC22 is involved in peroxisome fatty acid β-oxidation and/or IBA metabolism. Mutants deficient in fatty acid β-oxidation fail to convert stored lipid in seeds into energy, thus young seedlings are largely dependent on exogenous sucrose to become established as photosynthetic plants (Hu *et al.*, 2012). The conversion of IBA to IAA, a phytohormone that inhibits primary root growth, also occurs in the peroxisome through β-oxidation. Mutants defective in this process display reduced response to exogenous IBA and therefore the primary root length of mutant seedlings is not inhibited as much as the wild type in response to IBA (Zolman *et al.*, 2000).

ubc22 seedlings were grown under both light and dark conditions on 1/2MS plates with or without 0.5% (w/v) sucrose. Hypocotyl lengths of seedlings grown in the dark and root lengths of seedlings grown in the light were compared with wild-type seedlings grown in the same conditions (Figure 2.7). Both *ubc22* mutants showed no obvious difference from the WT plants in the sugar dependence assay (Figure 2.8),

indicating that peroxisomal fatty acid β-oxidation is not strongly affected in the absence of UBC22. Interestingly, the primary root lengths of 7-day old *ubc22-1* and *ubc22-2* seedlings were 33% and 26% respectively longer than that of Col-0 on medium with or without sucrose (Figure 2.7A).

To test whether *ubc22* mutants were compromised in IBA metabolism, we grew plants on 1/2MS plates that contained various concentrations of IBA. By comparing the relative root length of mutants on different IBA concentrations, we are able to test whether the efficacy of this pathway is changed. The root lengths of *ubc22-1* and *ubc22-2* lines decreased significantly in response to IBA, indicating that IBA metabolism was not impaired in *ubc22* mutants (Figure 2.9A). When compared with WT, the primary root length of both *ubc22* alleles decreased more rapidly as IBA concentration increased (Figure 2.9B). This result shows that the efficiency of IBA metabolism seems higher without UBC22, indicating that UBC22 might play a negative role in peroxisomal IBA metabolism.

2.4.6 Null *ubc22* mutants produce bigger plants and larger and heavier seeds that store a higher amount of protein and fatty acids

In addition to the longer primary roots, the size of the first true leaves of *ubc22-1* and *ubc22-2* was about 55% larger than that of Col-0 (Figure 2.10A). To examine this phenotype in more details, I grew mutants and Col-0 on three different media: plain medium with agar only, 1/2 LS (Linsmaier and Skoog) medium with sucrose, and 1/2 MS (Murashige and Skoog) medium with sucrose. Primary root growth of 3d to 7d plants was investigated. The growth rate of the primary root of the *ubc22* mutants was

lower than Col-0 when grown on plain and 0.5x LS medium, while they grew slightly faster than Col-0 when grown on 0.5x MS medium (Figure 2.11). From 3 to 7 days, the difference in primary root length and cotyledon size between null *UBC22* mutants and Col-0 was very obvious. On 0.5x LS medium, primary root length of 3-day-old mutants were about 40% longer than Col-0. This number decreased at 7 day, when *ubc22-1* and *ubc22-2* seedlings were 33% and 26% respectively longer than that of Col-0. These results suggest that the growth rate of Col-0 is faster than mutants when grown on 0.5x LS medium at early stage whereas when plants were grown on 0.5x MS medium, the growth rate of the primary root of the *ubc22-1* was similar to Col-0, and the growth rate of *ubc22-2* was 10% faster than Col-0. Finally, *ubc22* adult plants of both mutant lines are taller than Col-0, a phenotype that will need to be analyzed in more details in the future.

The size of plant organs is determined by both cell size and number (Hua and Chua, 2003). To determine which factor leads to the longer primary root phenotype in null *ubc22* mutants, I performed propidium iodide (PI) staining on 5-day-old seedlings to observe and measure the cell size and calculate cell number in roots. Cell size in the elongation zone and division zone in both *ubc22* lines was similar to Col-0 (Figure 2.12). Since both 5-day-old *ubc22* lines have longer primary root than Col-0, we conclude that the longer primary roots of the mutants is due to the possession of higher cell numbers in the roots.

These results prompted us to trace the phenotype back to the seeds, where the seedlings come from. Statistically significant differences were observed with respect to the size and weight of dry seeds between *ubc22* and Col-0. Seed length and width were

measured using over 100 seeds each time, using seeds from independent batches. Null *ubc22* mutant seeds were statistically larger in both length and width compared to Col-0 (Figure 2.13). I further measured the weight of seeds using 1000 seeds randomly selected from three independent batches. As shown in Figure 2.14A, null *ubc22* lines are about 45% heavier than Col-0 (Figure 2.14A).

The significant difference in size and weight between the seeds of null *ubc22* mutants and WT prompted me to analyze protein and fatty acid composition of seeds. *ubc22-1* and *ubc22-2* seeds contained ~36% more total protein than Col-0 (Figure 2.14B). Compared to the fatty acid composition of WT seeds, both mutant *ubc22-1* and *ubc2-2* have higher amount of 18:1, 18:2, 18:3 and 20:1 fatty acids and total FAME (fatty acid methyl esters); *ubc22-1* and *ubc22-2* contain 46% and 38% higher amount of total FAME than Col-0 (Figure 2.14C). The molar percentage of each type of fatty acids in *ubc22-1* and *ubc2-2* are similar to that in WT (Figure 2.14D). These data suggest that the larger size of *ubc22* mutant seeds might be due to the higher amount of stored nutrients such as lipids and proteins in the seeds.

2.4.7 Null *ubc22* mutants have reduced seed yield

To check further into seed development, siliques of the mutants were analyzed. Siliques of both *UBC22* knock out lines were about 33% shorter than Col-0 (Figure 2.15A). The number of seeds in each silique was 65% less than WT (Figure 2.15B). I further measured the total seed weight from a single plant, and found that the total seed weight of Col-0 per plant was about two times higher than that of the *UBC22* loss-of-function mutants. I calculated the approximate number of seeds and siliques on each

plant for each lines, and concluded that *ubc22-1* and *ubc22-2* yielded on average 63% and 66% fewer seeds, and 38% and 42% fewer siliques compared with the wild type. In summary, although each seed of null *UBC22* mutants is larger than Col-0, the total seed production is decreased in the absence of *UBC22*.

In plants, seed size and number are the most direct parameters for yield (Van Daele *et al.*, 2012). In nature, seed number is often negatively correlated with seed size (Alonso-Blanco *et al.*, 1999). In this work, both *ubc22* mutant lines produce substantially fewer seeds per plant, but the seeds are larger. This might be due to less competition between zygotes toward the limited carbon and other nutrients provided by the mother plant.

Given the mutant phenotypes in seed formation, I checked whether there is any pollen or pistil phenotype in the *ubc22* mutants. About two thirds of the ovules in dissected green siliques of *ubc22* mutants were unfertilized, and the distribution of the aborted ovules in the siliques was random (Figure 2.16). The total number of ovules in both null *ubc22* lines was similar to that in Col-0, indicating the low seed yield could be ascribed to the malfunction of pollen or pistil, or both. The viability of *ubc22-1* and *ubc22-2* mature pollen was investigated using Alexander's stain, which stained the pollen from both *ubc22* lines and Col-0 at similar red purple levels, indicating that the mutant pollen grains are as viable as those of the wild type (Figure 2.17). Further physiological examinations of pollen and the female gametophyte in *in vivo* conditions are underway.

2.3 DISCUSSION

The biological function of peroxisomes in plant reproduction was reported recently. The *Arabidopsis PEX13/AMC* gene is transiently expressed in male and female gametophytes during fertilization (Boisson-Dernier *et al.*, 2008). AMC functions as a peroxin essential for protein import into peroxisomes in gametophytes. An interesting phenomenon was discovered in the loss-of-function mutant of *AMC,* in which the pollen tube reception is impaired only when an *amc* pollen tube reaches an *amc* female gametophyte, resulting in pollen-tube overgrowth and failure to release sperm cells. Another *Arabidopsis* peroxisomal gene involved in plant reproduction is *DAU,* which encodes a peroxisomal membrane protein ABERRANT PEROXISOME MORPHOLOGY9 (APEM9) that is transiently expressed from bi-cellular pollen to mature pollen during male gametogenesis. In plants, APEM9 is an integral peroxisomal membrane protein that functions as membrane anchor for PEX1 and PEX6 (Goto *et al*., 2011). In *dau* pollen, peroxisome biogenesis and peroxisomal protein import are impaired and JA level is significantly decreased (Li *et al.*, 2014).

In this work, I discovered that UBC22 is required for some aspects of *Arabidopsis* seed formation, because lack of a functional UBC22 dramatically decreases seed yield per plant. The seed yield per plant is a vital trait for grain crop cultivars, and thus it will be important to find out the biological mechanism of how UBC22 affects seed production in *Arabidopsis*. Crop seeds are the major resources of food and nutrition for human beings. Amino acid similarity-based searches in *Zea mays* (maize)*, Glycine max* (soybean)*, Oryza sativa* (rice) and *Triticum aestivum* (wheat) databases using AtUBC22 showed that maize, rice and soybean contain putative ubiquitin-conjugating enzyme

family proteins that respectively share 69%, 70% and 74% amino acid identity with AtUBC22. Interestingly, all three putative UBC22 orthologous proteins possess a KRL> tripeptide at the C-terminal end (Figure 2.18). This result indicates that UBC22 is a plant-specific peroxisomal protein that may carry out function that of potential values to agriculture.

Although we have proved that *Arabidopsis* UBC22 is targeted to the peroxisomes, we do not have sufficient knowledge to relate the low reproduction rate displayed in the mutants to the dysfunction of peroxisomes. We cannot exclude the possibility that UBC22 may also target to other organelles besides peroxisomes to fulfill its function.

To date, our understanding about the role of peroxisomal localized E2 in peroxisome biogenesis and metabolic functions is still scarce. In *Arabidopsis*, PEX4 was the only E2 known to be associated with peroxisomes before the identification of UBC22. Yeast Pex4p binds to the peroxisomal membrane via its membrane anchor Pex22p, and was shown in *vitro* to mono-ubiquitinate Pex5p during receptor export (Platta *et al.*, 2007). Yeast *S. cerevisiae* Ubc4p, Ubc5p and Ubc1p are E2 enzymes involved in the polyubiquitination of Pex5p (Kragt *et al.*, 2005; Kiel *et al.*, 2004). A previous *in vitro* study of AtUBC22 shows that UBC22 is able to form poly-ubiquitin chains in the absence of an E3 (Kraft *et al.*, 2005). However, although *in vitro* assays shows UBC22 to have E3-independent polyubiquitination activity, one has to investigate *in planta* to determine whether UBC22 collaborates with an E3 or directly transfers mono- or poly-ubiquitin chains to its substrates in an E3-independent manner.

In peroxisomes, the four-carbon IBA is converted to the two-carbon IAA in a mechanism similar to fatty acid ß-oxidation (Zolman and Bartel, 2004; Zolman *et al.*, 2001). Mutants of the fatty acid ß-oxidation pathway such as *aim1 and ped1/kat2* are also resistant to exogenous IBA, while *ibr1, ibr3, ibr10* only show IBA resistant phenotypes, suggesting that these enzymes might be specific for IBA-CoA ß-oxidation. Our sucrose dependence experiments suggest that the peroxisomal fatty acid β-oxidation pathway is not strongly affected in the absence of UBC22 (Figure 2.8). In the IBA resistant assay, IBA seems more efficient in both *ubc22* mutant lines compared to Col-0, indicating that UBC22 might act as a negative regulator in peroxisomal IBA conversion. Since fatty acid β-oxidation is unaffected in null *UBC22* mutants, we speculate that UBC22 might be involved in the regulation of IBA metabolism through modulating the activities of IBA pathway-specific enzymes, such as IBR1, IBR3 and IBR10.

I also report that two *UBC22* knock out lines produce fewer but larger seeds. The higher weight of null *UBC22* mutant seeds might be due to less competition between zygotes for nutrients due to the aborted ovules. Mature seeds of null *ubc22* mutant lines are equally scattered inside siliques, indicating that the length of mutant pollen tubes is likely to be normal. Further *in vivo* analysis of the loss-of-function mutants, such as in vivo pollen tube growth assay and reciprocal cross-pollinations between wild-type and *ubc22* plants, needs to be done to elucidate the mechanism behind this phenotype.

In summary, I have characterized a novel Arabidopsis peroxisomal protein, AtUBC22, whose function might be conserved in diverse plant species such as food

crops maize, rice and soybean. Morphological and physiological analysis of null *ubc22* mutants reveals that UBC22 has an effect on seed formation and plant growth and that UBC22 might act as a negative regulator of peroxisomal IBA metabolism. We speculate that UBC22 affects seed yield by exerting its function inside peroxisomes. It is possible that certain UBC22-related peroxisomal pathways are linked to male or female gametophytic physiological activities, which then further affect plant reproduction. However, many questions remain to be answered. For example, which peroxisomal pathway is UBC22 involved in? What is the physiological and molecular mechanism behind the unfertilized ovules? How are peroxisomes linked to the decreased seed yield phenotype?

Table 2.1 *Arabidopsis* UBCc domain-containing proteins

	Accession#	Protein	Last three a.a. at C-terminal
1	AT1G14400	UBC1	TAD>
2	AT1G16890	UBC36,UBC13B	SGA>
3	AT1G17280	UBC34	LQL>
4	AT1G36340	UBC31	ANN>
5	AT1G45050	UBC15	DKV>
6	AT1G50490	UBC20	PSA>
7	AT1G53020	UBC26, PFU3	SSR>
8	AT1G53023	Ubiquitin-conjugating enzyme family protein	CSV>
9	AT1G53025	Ubiquitin-conjugating enzyme family protein	SSR>
10	AT1G63800	UBC5	LDP>
11	AT1G64230	UBC28	AMG>
12	AT1G75440	UBC16	DKV>
13	AT1G78870	UBC35,UBC13A	SGA>
14	AT2G02760	UBC2	TAD>
15	AT2G16740	UBC29	ALF>
16	AT2G16920	UBC23,PFU2	QQQ>
17	AT2G33770	UBC24,PHO2	PES>
18	At2G46030	UBC6	ADP>
19	AT3G08690	UBC11	AMG>
20	AT3G08700	UBC12	AMG>
21	AT3G12400	ATELC, ELC	LHS>
22	AT3G12775	Ubiquitin-conjugating enzyme family protein	SFD>
23	AT3G13550	CIN4,COP10,EMB144,FUSCA 9	FAK>
24	AT3G15355	UBC25,PFU1	SSS>
25	AT3G17000	UBC32	DQS>
26	AT3G20060	UBC19	LNA>
27	AT3G24515	UBC37	CRP>
28	AT3G46460	UBC13	EMF>
29	AT3G52560	MMZ4,UEV1D,UEV1D-4	TCF>
30	AT3G55380	UBC14	EML>
31	AT3G57870	AHUS5,ATSCE1,EMB1637,SCE1,SCE1A	ALV>
32	AT3G59410	ATGCN2, GCN2	VWS>
33	AT3G60300	RWD domain-containing protein	GDK>
34	AT4G27030	FAD4, FADA	NQA>
35	AT4G27960	UBC9	AMG>
36	AT4G36410	UBC17	DKV>
37	AT4G36800	RCE1	RCI>
38	AT5G05080	UBC22	KRL>
39	AT5G13860	ELC-LIKE, ELCH-LIKE	LHS>

Table 2.1 cont'd

40	AT5G25760	UBC21,PEX4	KKG>
41	AT5G41340	UBC4	PDP>
42	AT5G41700	UBC8	AMG>
43	AT5G42990	UBC18	DKV>
44	AT5G50430	UBC33	LQL>
45	AT5G50870	UBC27	CSA>
46	AT5G53300	UBC10	AMG>
47	AT5G56150	UBC30	AMG>
48	AT5G59300	UBC7	EMF>
49	AT5G62540	UBC3	SYV>

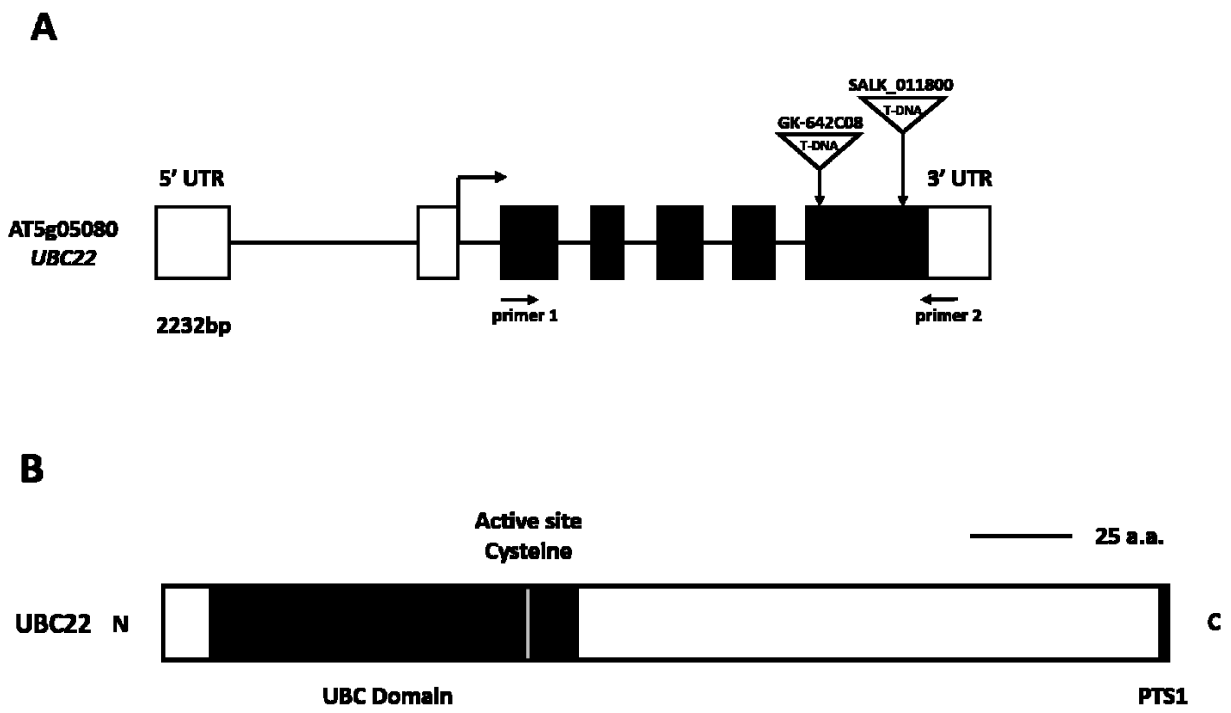

Figure 2.1 Sequence and structural analysis of UBC22.
(A) Genomic structure of *UBC22*. The T-DNA insertion sites in *ubc22-1* (GK-642C08) and *ubc22-2* (SALK_011800) are indicated.
(B) Putative protein structure of UBC22. UBC domain, Ubiquitin Conjugating domain; PTS1, Peroxisome Targeting Signal type 1.

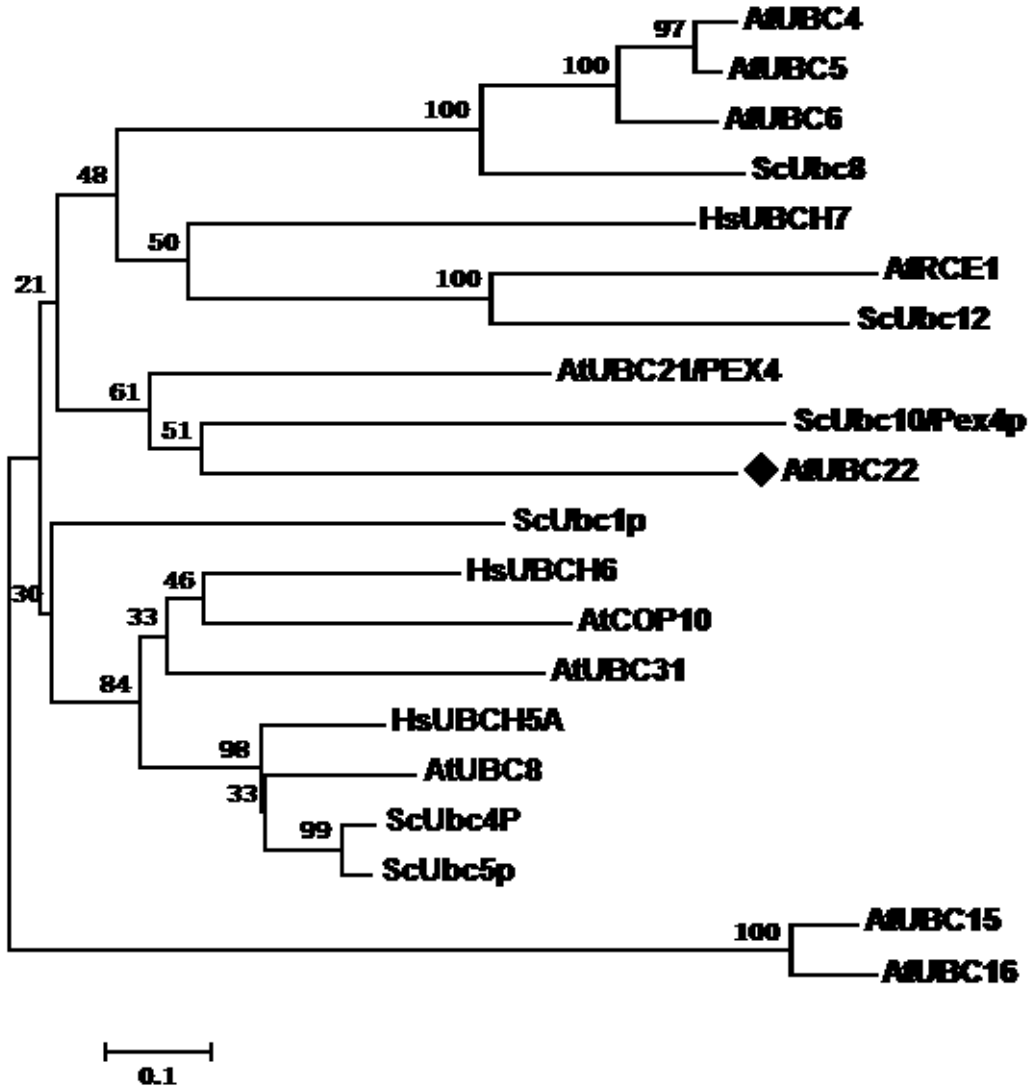

Figure 2.2 Phylogenetic analysis of *Arabidopsis* UBC22.
Phylogenetic analysis of the relationship between Arabidopsis UBCs and the six known yeast UBCs and three known human UBCs. Scale bar, 0.1 amino acid substitutions per site. Bootstrap was performed from 1000 replicates. Bootstrap values are shown at the tree nodes.

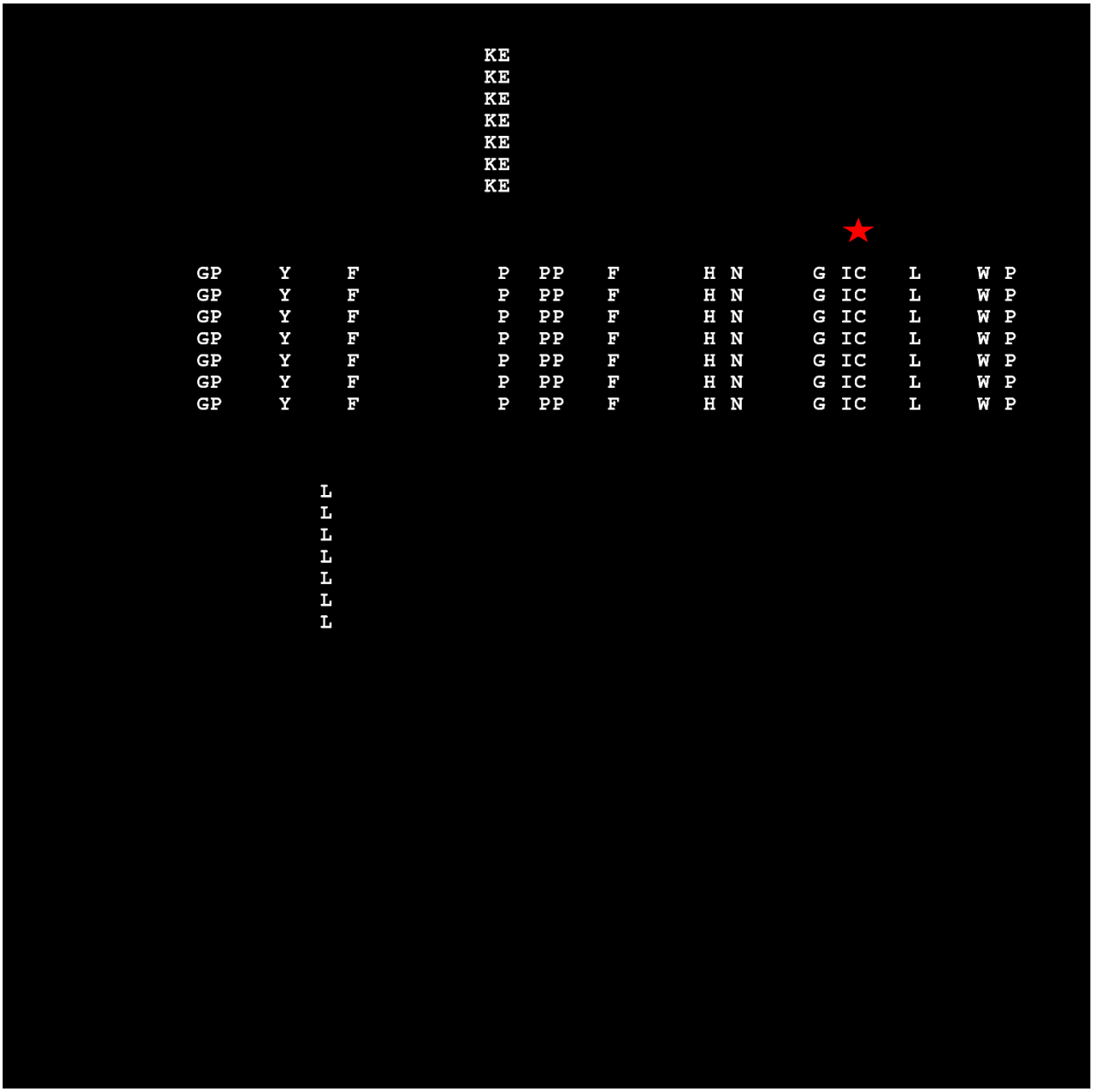

Figure 2.3 Amino acid sequence alignment of *Arabidopsis* UBC22 and homologous sequences.
Sc, *S. cerevisiae;* Hs, *Homo sapiens*. Full amino acid regions from human UBCH5A (HsUBC5A), *Arabidopsis thaliana* UBC22 (AtUBC22) and PEX4 (AtPEX4), *S. cerevisiae* Ubc1p (ScUbc1p), Ubc4p (ScUbc4p), Ubc5p (ScUbc5p) were aligned using ClustalW2. Identical residues are shaded. Conserved sequences are indicated by black boxes. Red asterisk indicates the conserved active site Cys residue.

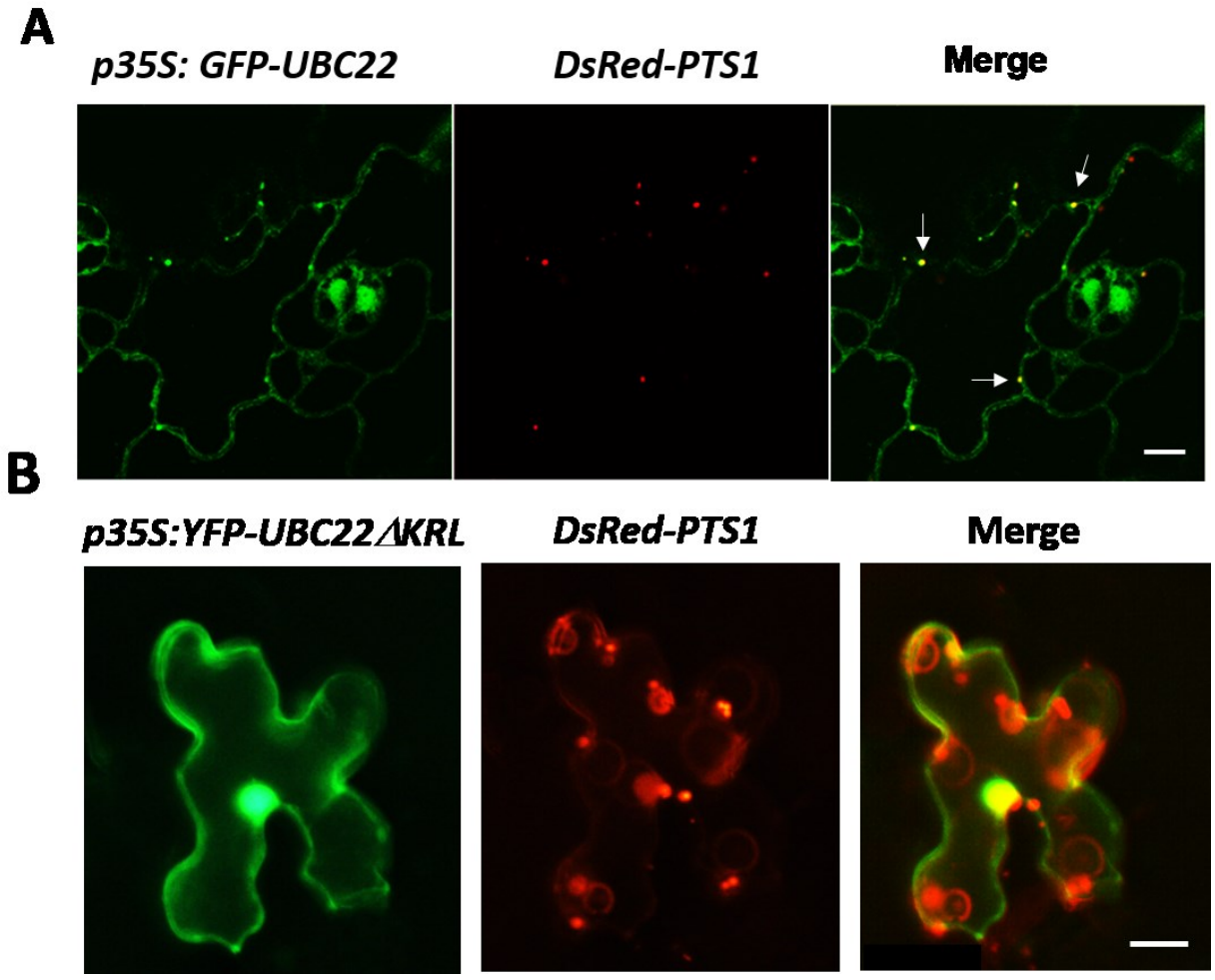

Figure 2.4 UBC22 localizes to the peroxisome through a C-terminal PTS1 (KRL>). (A) Confocal images of 35S::GFP-UBC22 (green) co-expressed with the peroxisome marker 35::DsRed-PTS1 (red) in leaf epidermal cells of Arabidopsis transgenic plants. Scale bar = 10 μm. White arrow indicate co-localization of UBC22 and peroxisomes.

(B) Epifluorescence images of 35S::YFP-UBC22ΔKRL (green) co-expressed with DsRedPTS1 (red) in tobacco epidermal cells. Scale bar = 10 μm

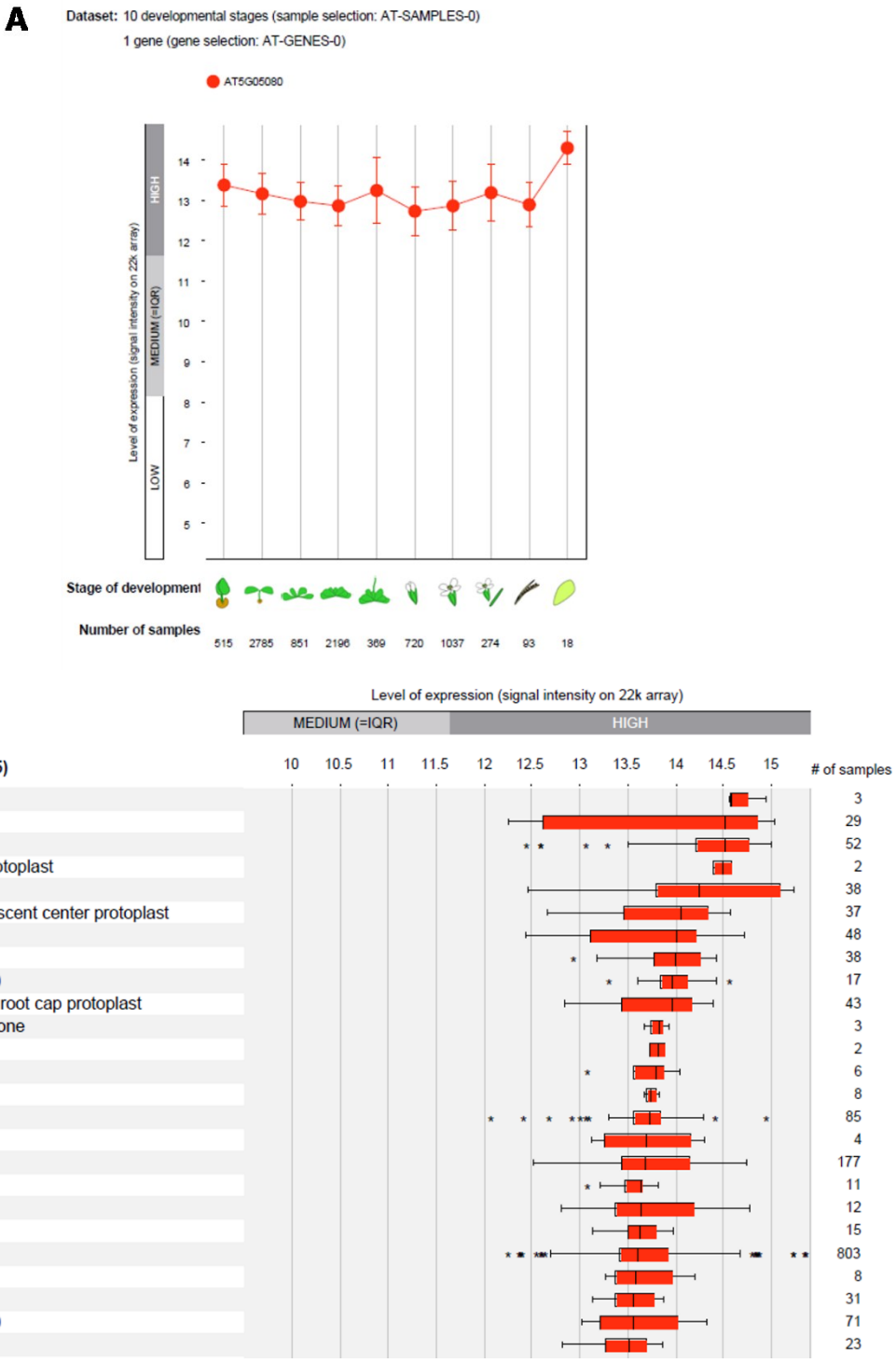

Figure 2.5 Expression patterns of *UBC22* in *Arabidopsis*

Figure 2.5 cont'd

(A) Expression at successive developmental stages. Y axis indicates the level of gene expression. Data used for the analysis were retrieved from GENEVESTIGATOR.
(B) Ranking of *UBC22* gene expression levels in various plant tissues.

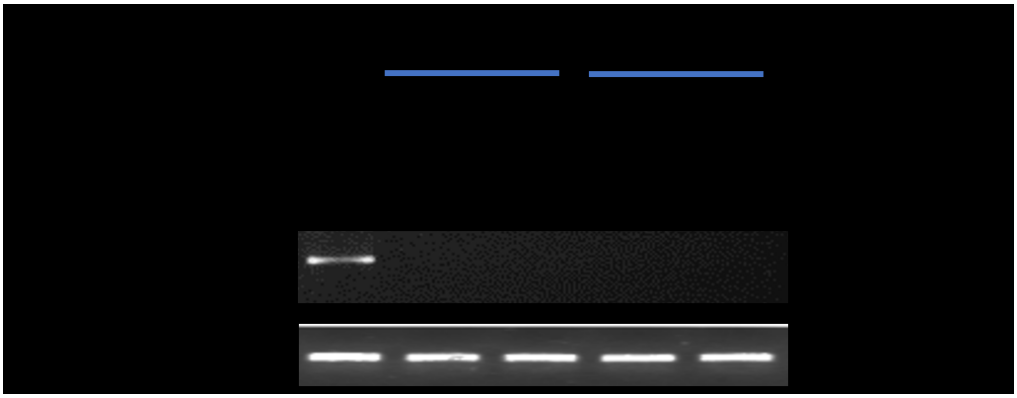

Figure 2.6 Expression level of *UBC22* in *Arabidopsis*
RT-PCR analyses of total RNA extracted from 10d seedlings of wild-type, and leaves and flowers from 10d seedlings and 8-week loss-of-function mutants (*ubc22-1* and *ubc22-2*) respectively. Primers used are indicated in Fig. 2.1A. The *UBQ10* transcripts are used as loading controls.

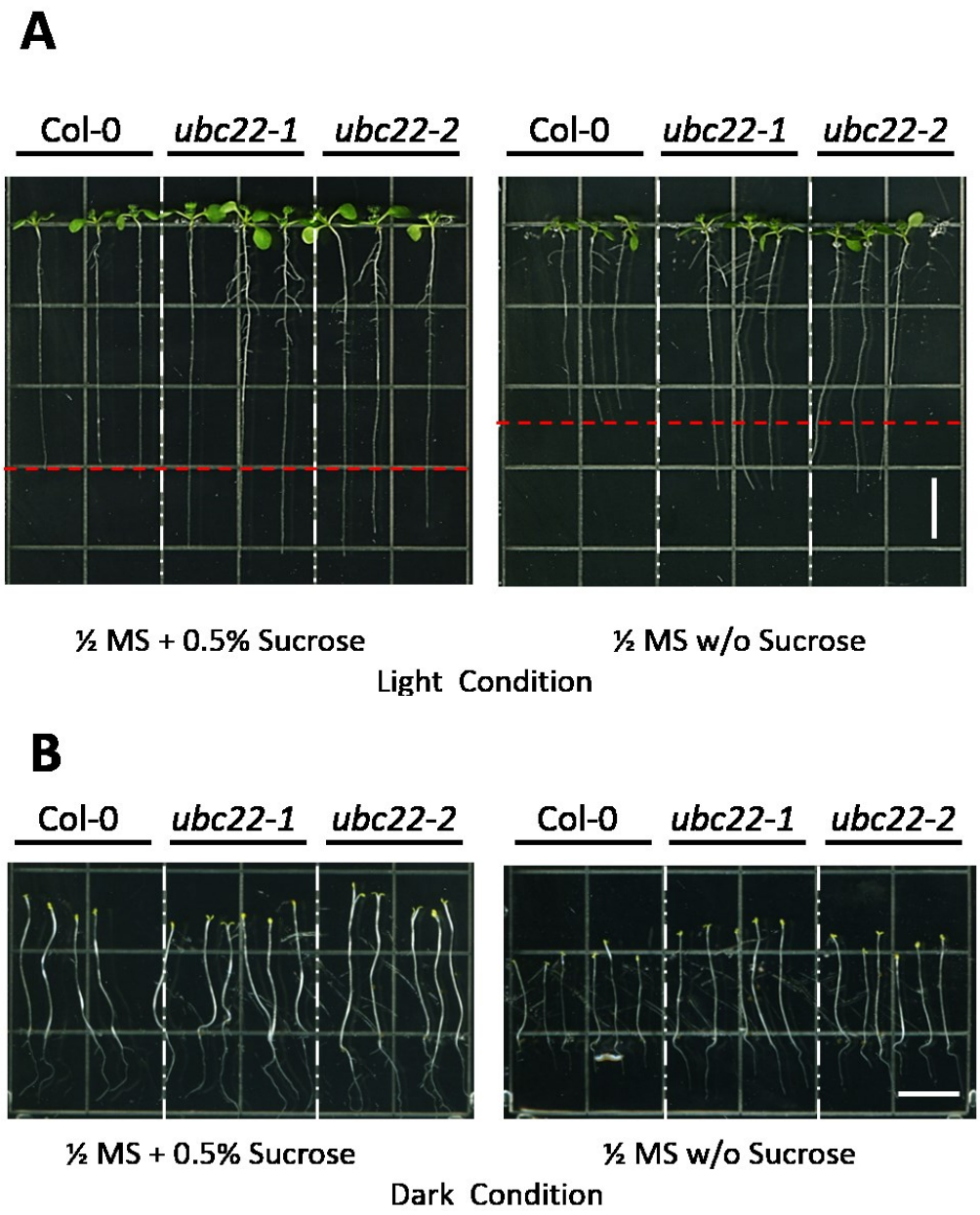

Figure 2.7 Sucrose-dependence assays on the *ubc22* mutants.
(A) Seven-day light-grown *seedlings*. Scale bar = 10 mm
(B) Seven-day dark-grown seedlings. Scale bar = 10 mm

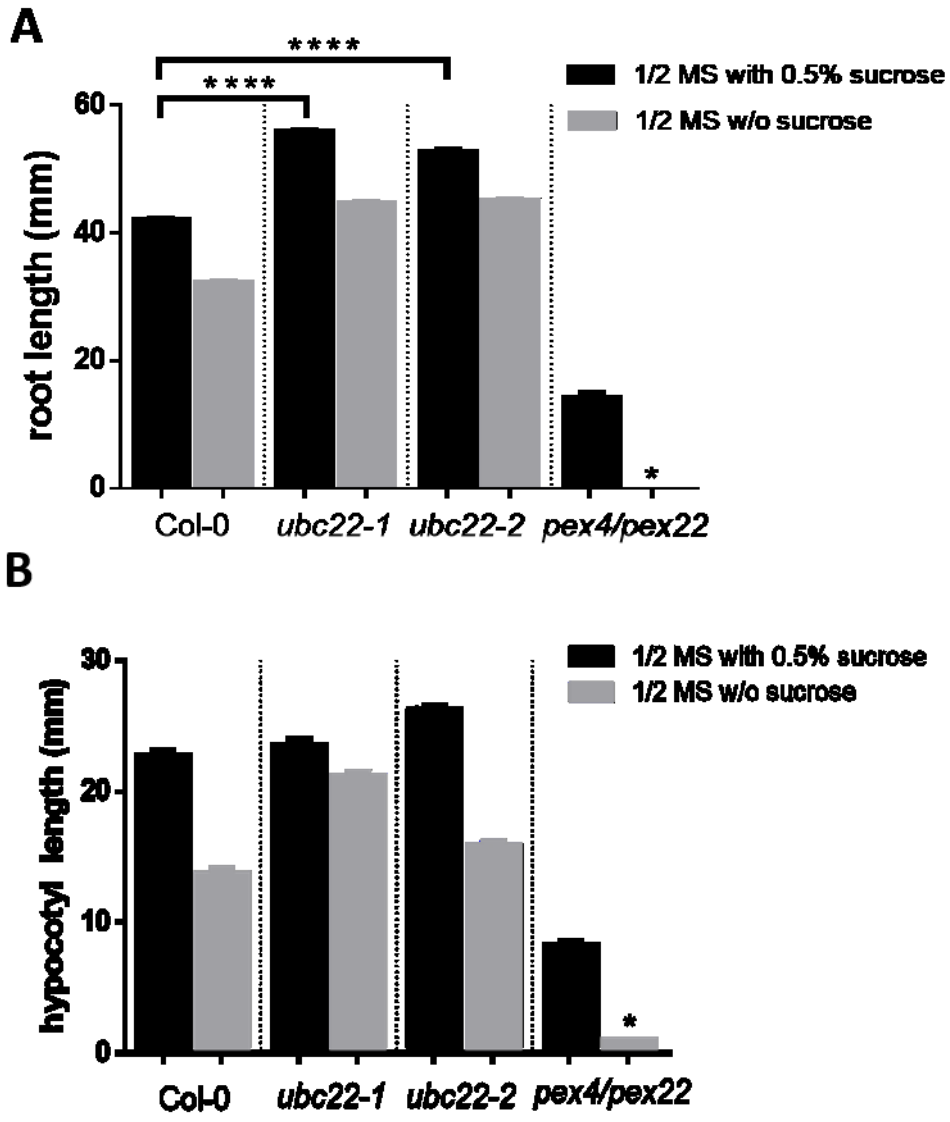

Figure 2.8 Quantification of root (A) and hypocotyl (B) lengths of seedlings in the sucrose dependence assay.
The *pex4 pex22* double mutant defective in peroxisome biogenesis was used as a positive control. Error bars represent SE. Asterisk indicates statistically significant differences between mutants and Col-0 under the same condition (Student's t-test, $p<0.0001$).

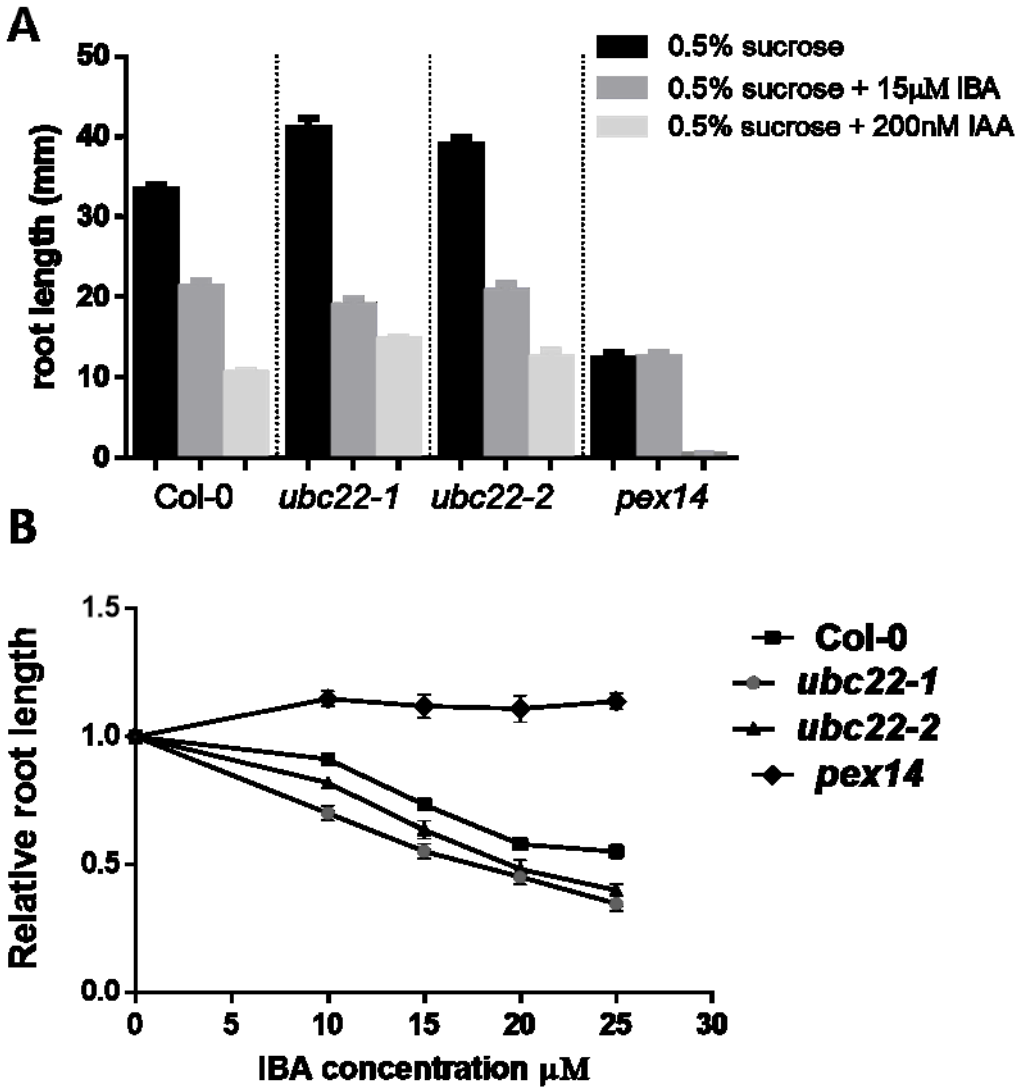

Figure 2.9 *ubc22* mutants are hypersensitive to IBA.

(A) Root lengths of 7-day-old seedlings grown on 1/2MS media with 15μm IBA or 200nm IAA were quantified. *pex14* was used as a positive control. Error bars represent SE (n> 40 for each genotype).

(B) Root lengths of 7-day-old seedlings grown on 1/2MS media with indicated concentration of IBA normalized to their respective average seedling root length growth on media without IBA. *pex14* was used as a positive control.

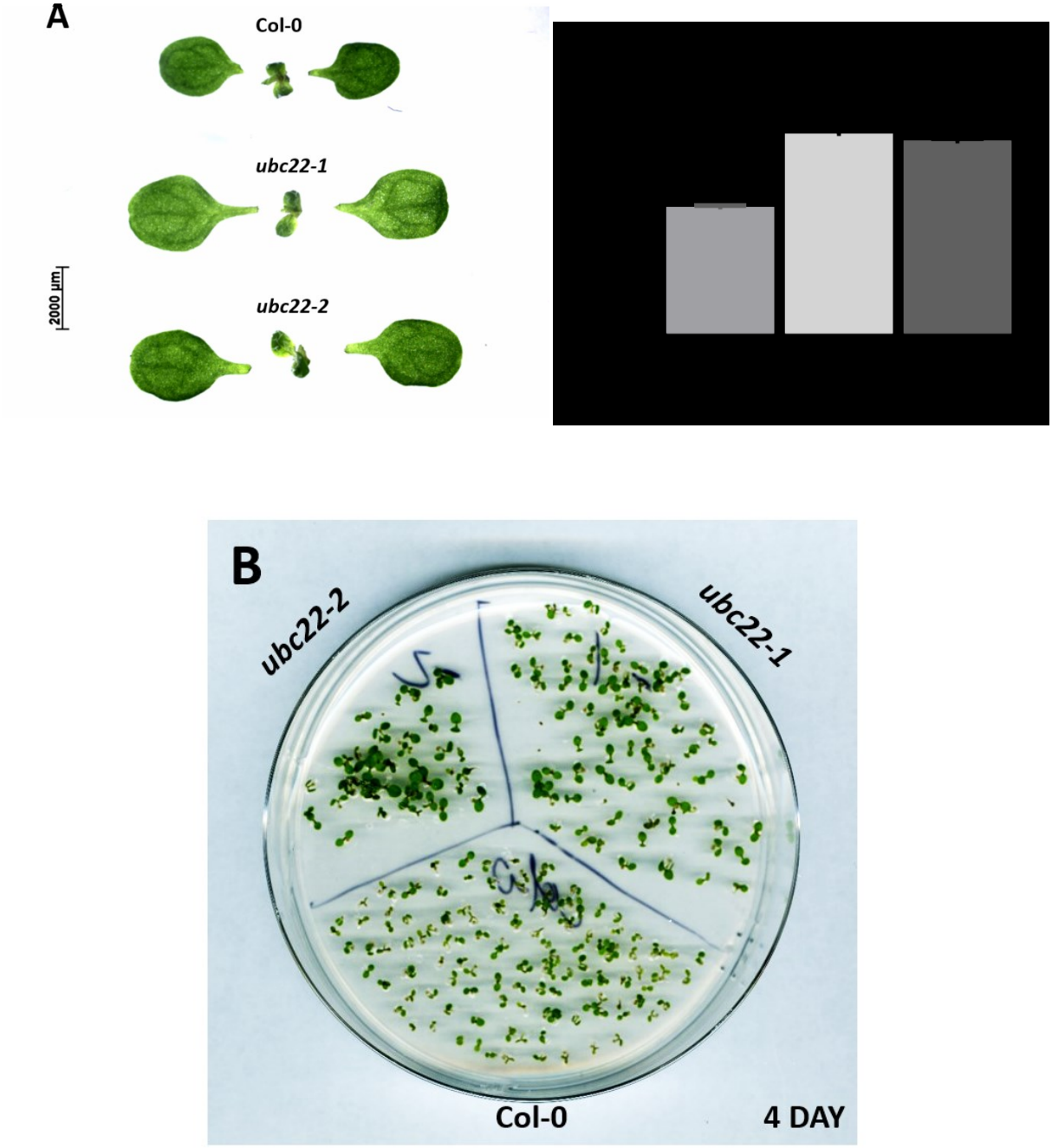

Figure 2.10 Arabidopsis *ubc22* have larger first true leaves and cotyledons

(A) True leaf size of 7-day-old seedlings grown on 1/2LS media 0.5% sucrose under light conditions. Left panel, image of representative seedlings, scale bar = 2mm. Right panel, average true leaves size.
(B) Four-day old seedlings of Col-0, *ubc22*-1and *ubc22-2.* Seedlings were grown on 1/2LS media with 0.5% sucrose under light conditions.

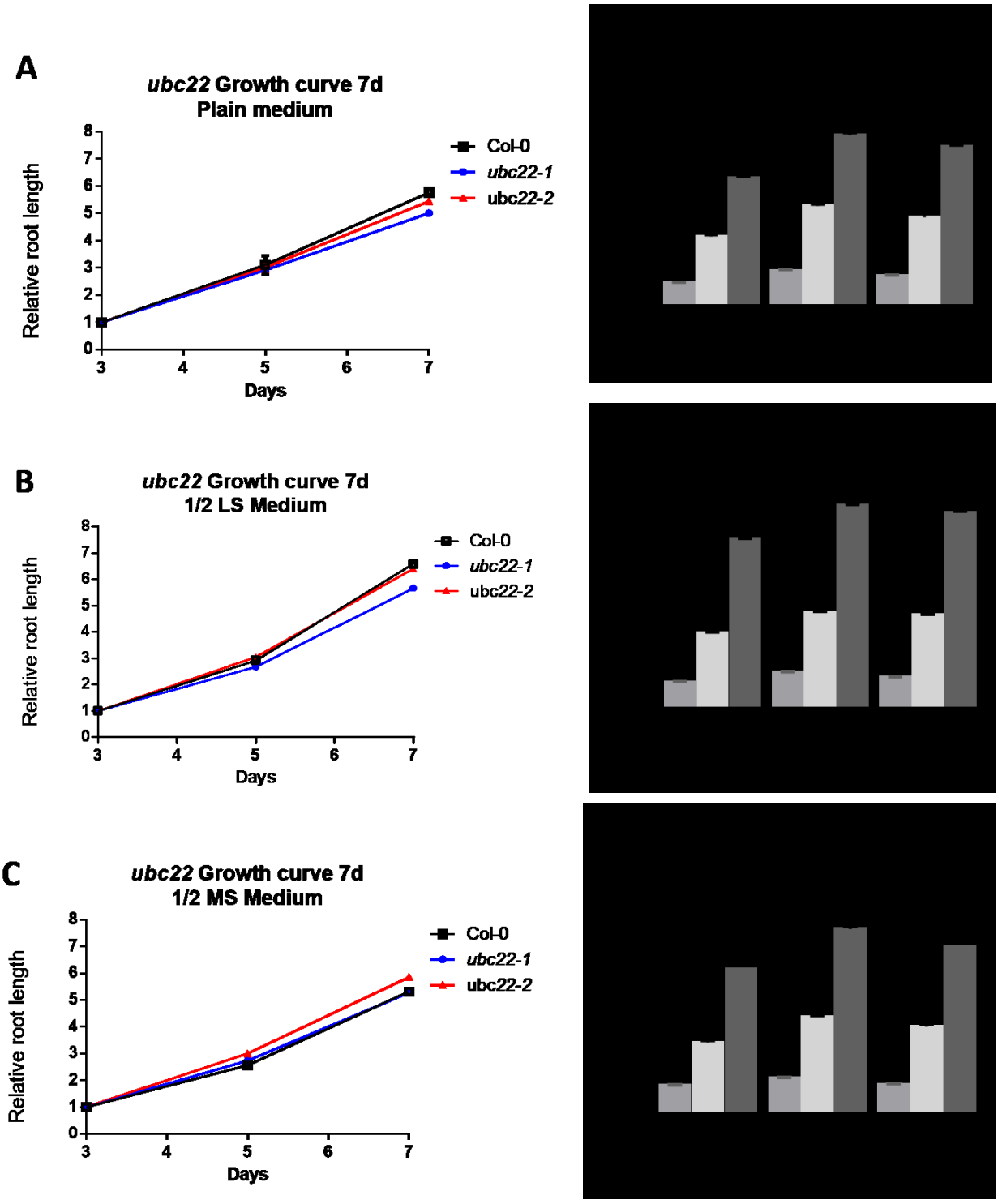

Figure 2.11 *Arabidopsis ubc22* have similar primary root growth rate to Col-0

Figure 2.11 Cont.
Relative root length of 3, 5 and 7-day-old *ubc22-1, ubc22-2* and Col-0 seedlings grown on (A) plain media with agar only, (B) ½ LS media with 0.5% sucrose and (C) 1/2 MS media with 0.5% sucrose was measured. Error bars indicate SE. Samples of each line > 30.

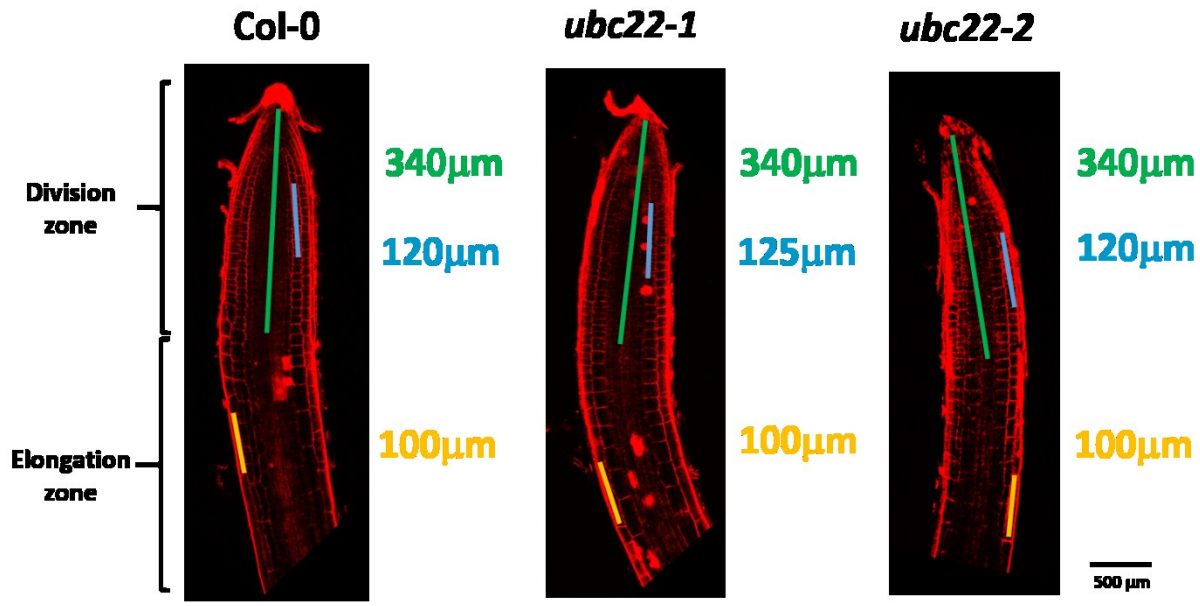

Figure 2.12 Comparison of root cell size between *ubc22* and Col-0.

Roots of 5-day-old wild type, *ubc22-1, and ubc22-2* were stained with propidium iodide (PI) to visualize the cell wall. Bar = 100 µm.

Green bar indicates the length of the division zone. Blue bar indicates the length of 10 cells in the division zone. Yellow bar indicates the length of one cell in the elongation zone.

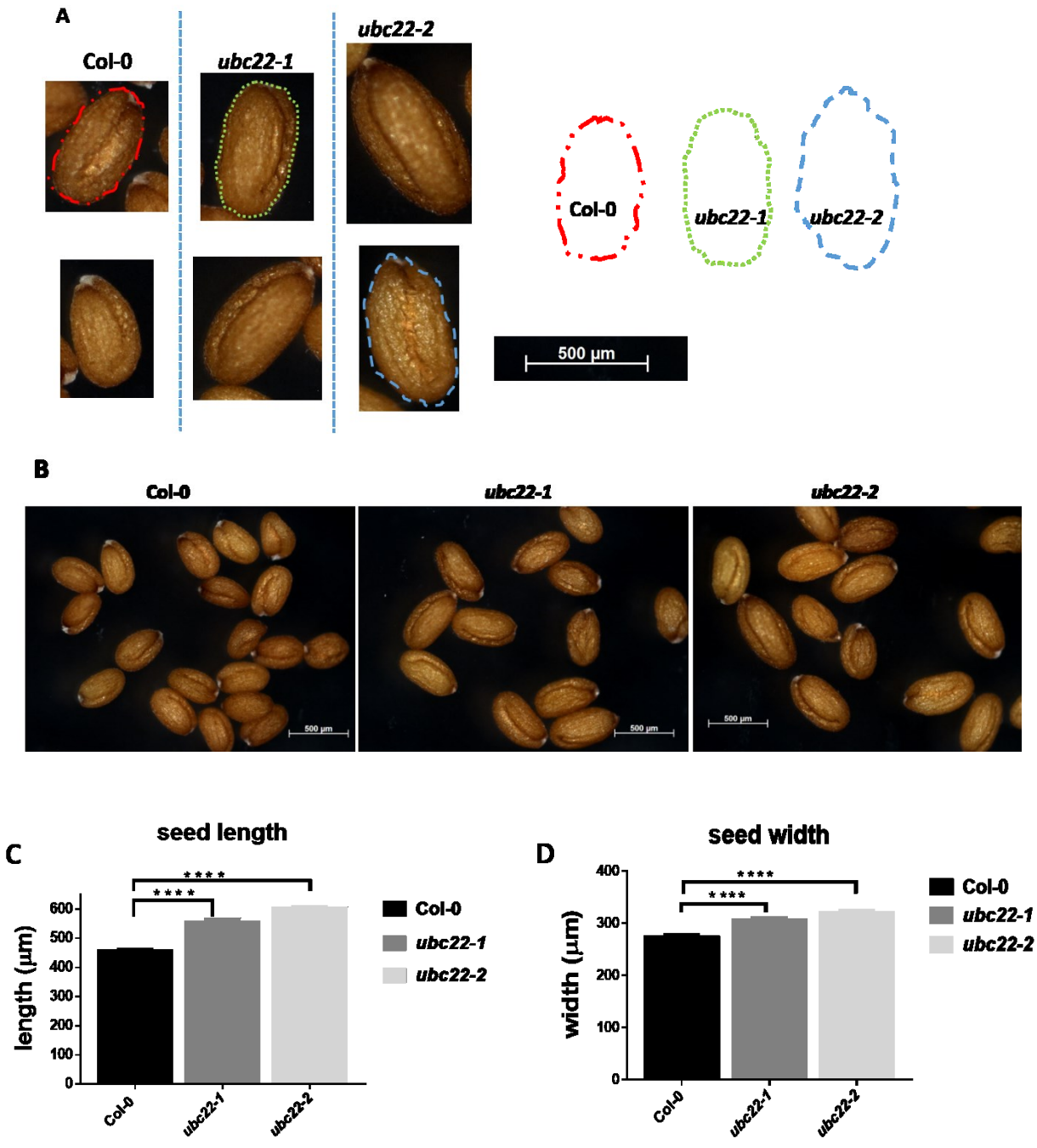

Figure 2.13 Morphological analysis of *ubc22* seeds.

Figure 2.13 cont'd
(A)(B) Dry seeds observed under the light microscope. Bar = 500 μm.
(C)(D) Lengths and widths of *ubc22* and Col-0 seeds. >100 seeds were measured. Asterisk indicates statistically significant differences between mutants and Col-0 (Student's t-test, $p<0.001$).

C

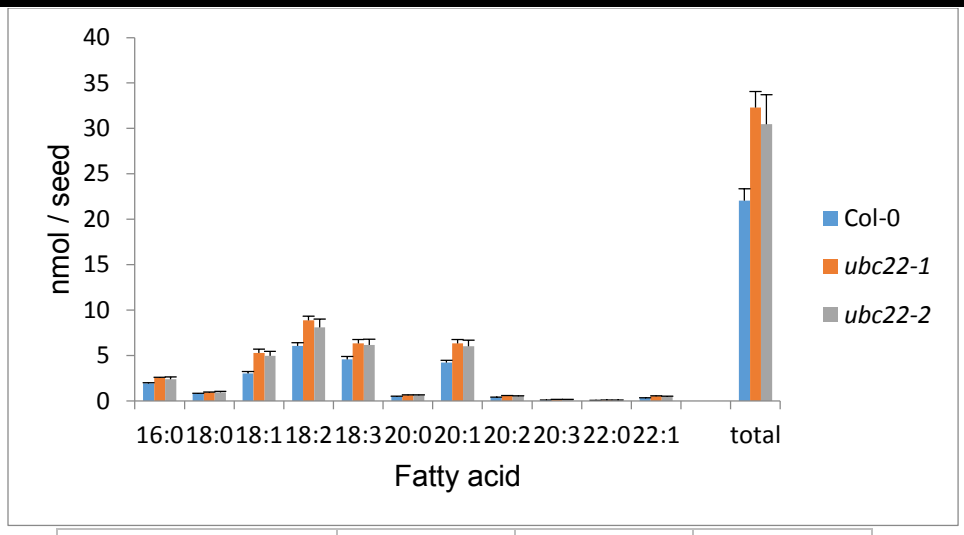

	Col-0	*ubc22-1*	*ubc22-2*
total (nmol/ seed)	22.052655	32.2887	30.4673

D

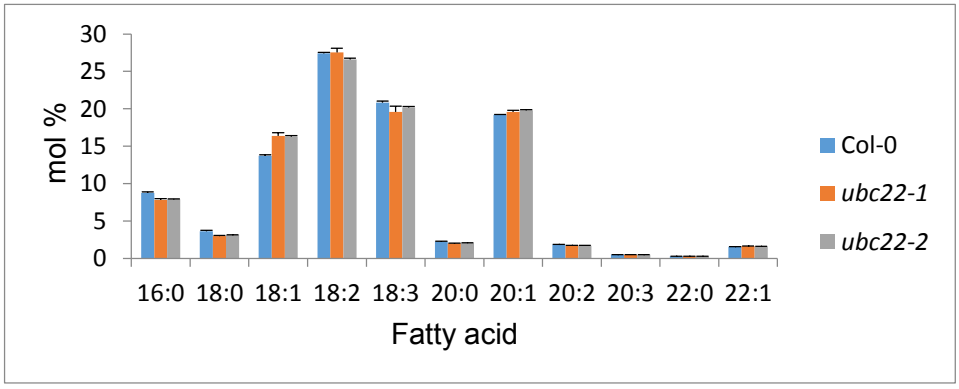

Figure 2.14 Analysis of the weight, protein content and fatty acids of *ubc22* mutants

Figure 2.14 cont'd
(A) Comparison of the average weight of 1000 seeds from *ubc22* mutants and Col-0. Seeds are from three independent batches
(B) Total protein content in 100 seeds from each genotype. Four asterisks indicate statistically significant differences between mutants and Col-0 (Student's t-test, $p<0.01$). Error bars represent SE
(C) Total fatty acid content in seeds of WT and *ubc22* mutants. Error bars represent standard deviation.
(D) Fatty acid composition analysis in seeds. Error bars represent standard deviation.

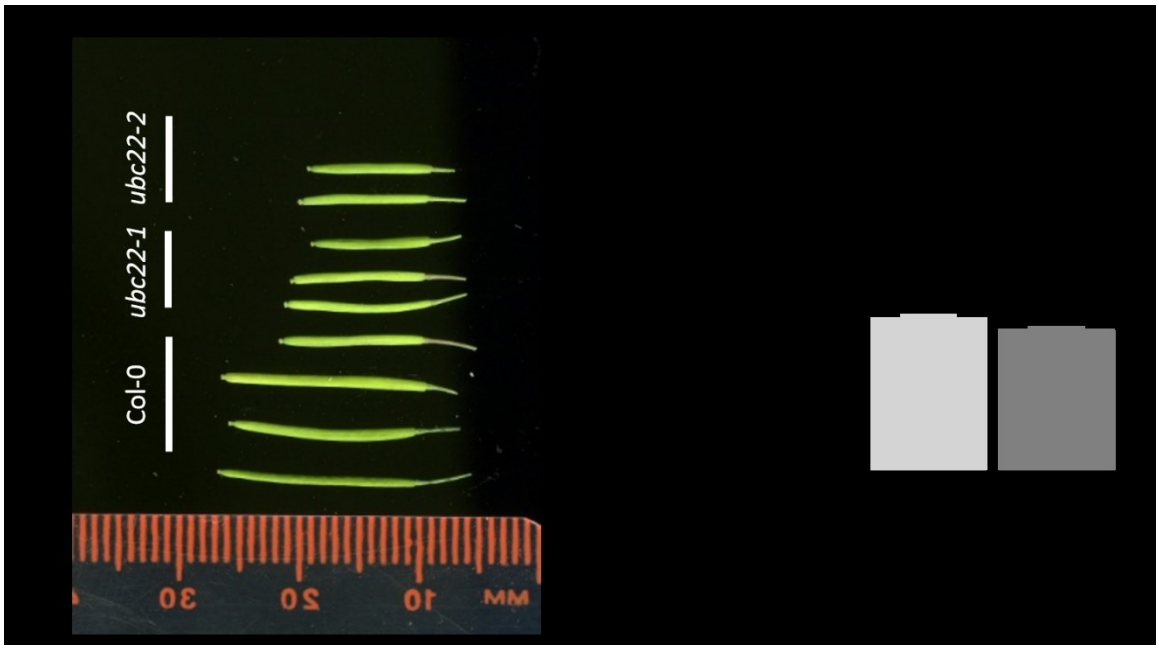

B

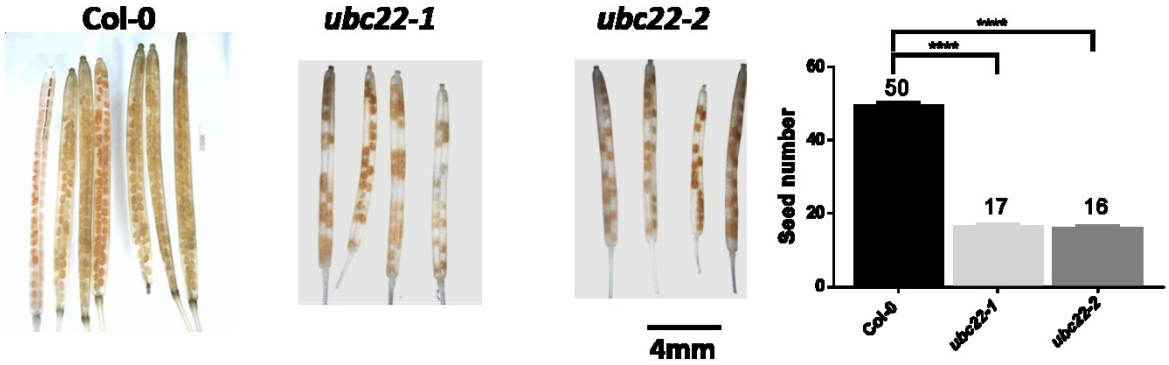

Figure 2.15 Silique analysis of *ubc22* mutants.

(A) Green siliques from 10-week plants. Silique lengths were measured using >30 siliques from each genotype. Asterisk indicates statistically significant differences between mutants and Col-0 (Student's t-test, $p<0.0001$).
(B) Comparison of seeds in the siliques of Col-0, *ubc22*-1and *ubc22-2*. The number of seeds per silique was counted using over 40 siliques from independent batches. Asterisk indicates statistically significant differences between mutants and Col-0 (Student's t-test, $p<0.0001$). Bar = 2 mm. Pictures are from representative siliques from each line.

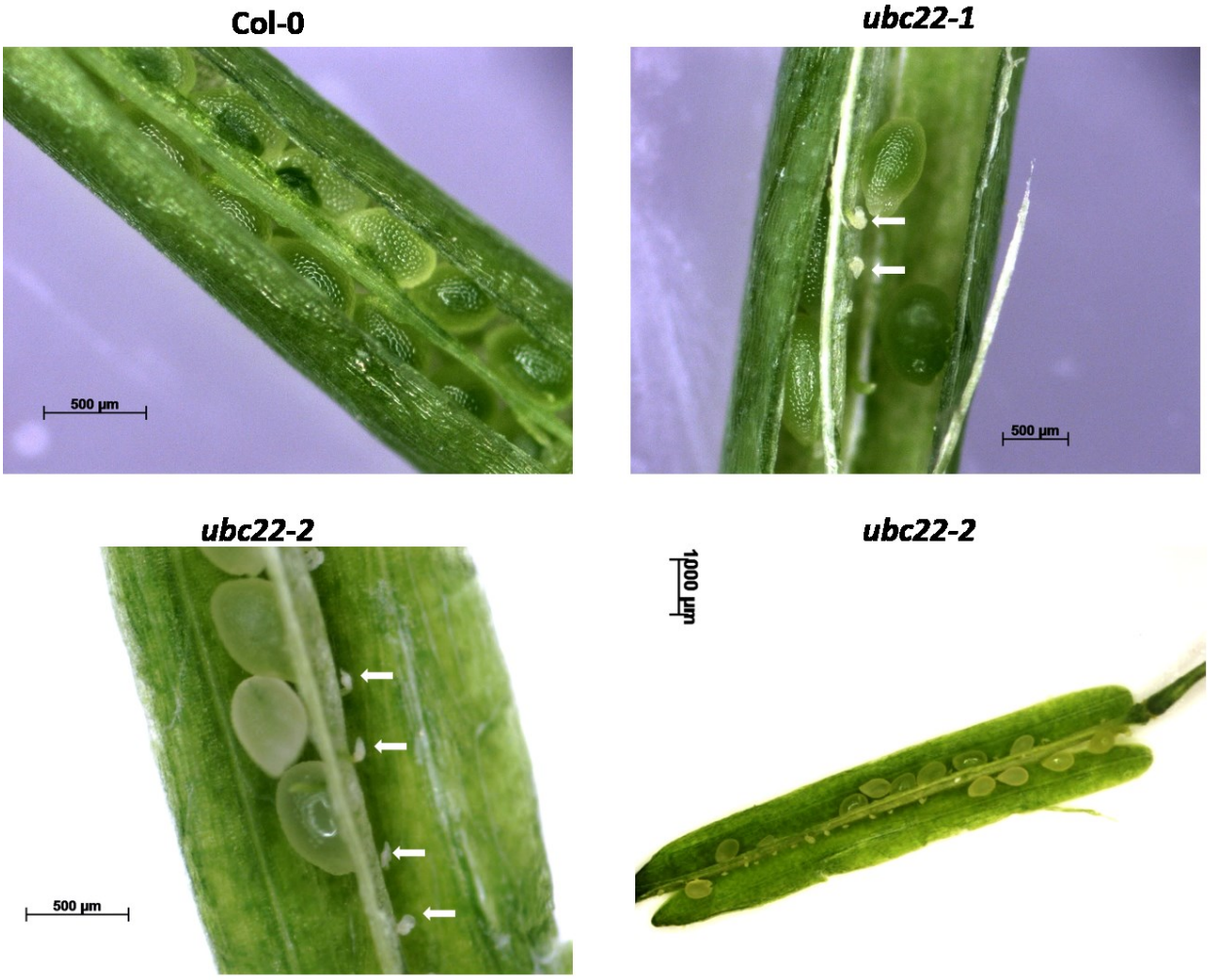

Figure 2.16 Unfertilized ovules of *ubc22* mutants in the silique.
Pictures are from representative siliques from each line. White arrows indicate unfertilized ovules. From left to right are Col-0, *ubc22-1, ubc22-1.*

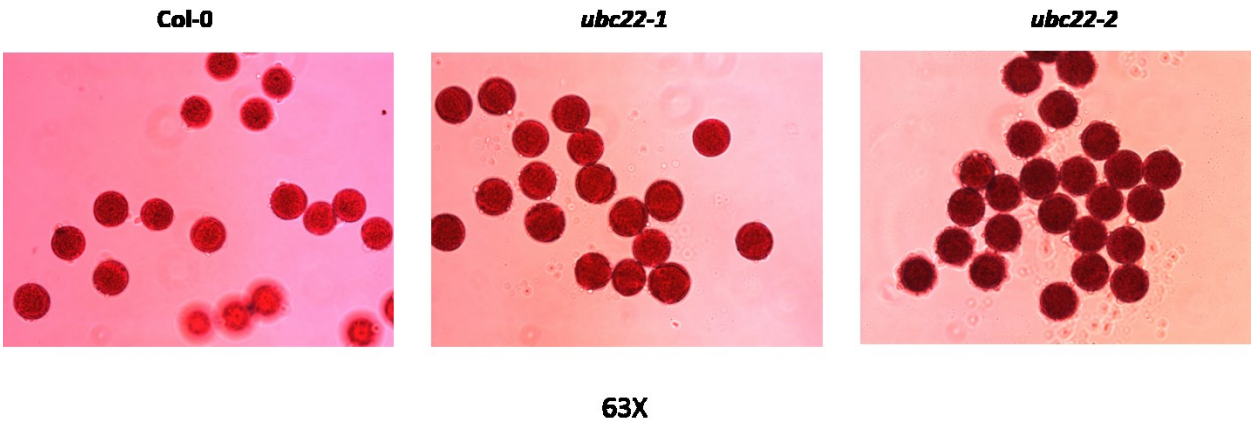

Figure 2.17 *in vitro* pollen viability test by Alexander staining
Non-aborted pollen grain stained red, aborted pollen grain were colorless or shows pale-green color.

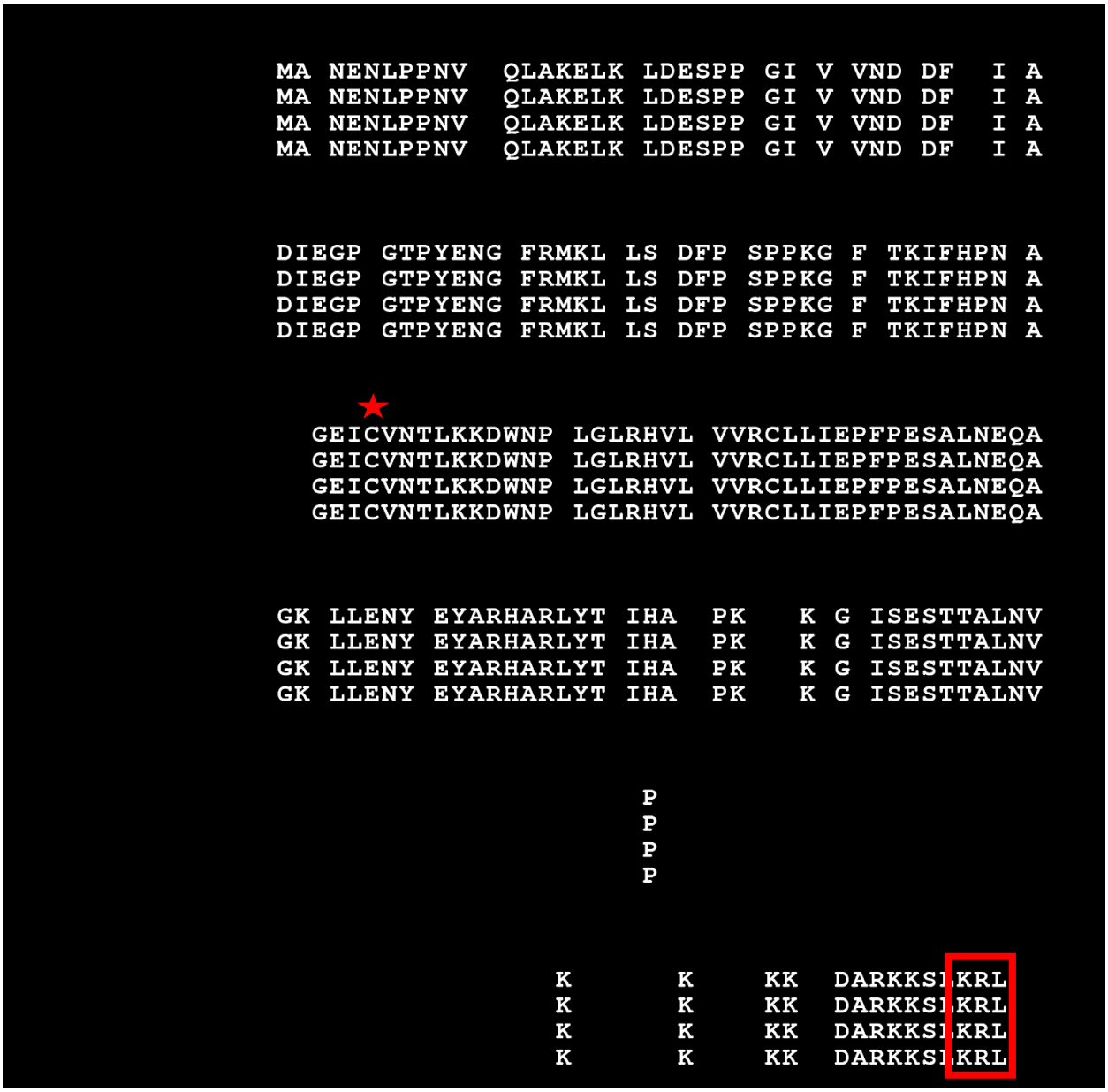

Figure 2.18 Amino acid sequence alignment of *Arabidopsis* UBC22 and its putative homologues in other species.

Amino acid sequence alignment of AtUBC22 and *Zea mays* UBCE2s (gb|ACG34027.1), *Oryza sativa* Os06g0660700 (*Japonica Group*, ref|NP_001058271.1), *Glycine max* UBCE2S (ref|XP_006604289). Conserved sequences are indicated by black boxes. Red asterisk indicates the conserved active site cysteine residue. Red box indicates the C-terminal peroxisome targeting signal tri-peptide KRL>.

2.4 METHODS

2.4.1 Plant material, growth conditions, and plant transformation

Arabidopsis (Arabidopsis thaliana) seeds were sown on ½ Linsmairer and Skoog medium (LS) medium containing 0.5% (w/v) sucrose. Plants were grown at 20°C with 70% humidity, under white light illumination at 70 to 80 μmol m^{-2} s^{-2} for 14h per day. Homozygous T-DNA insertion alleles *ubc22-1* (GK-642C08) and *ubc22-2* (SALK_011800) were obtained from GABI-KAT and ABRC (Arabidopsis Biological Recourse Center) respectively, both in Col-0 background. T-DNA insertion and the homozygosity of mutants were confirmed by PCR-based screening of genomic DNA. *UBC22* transcripts level was determined by reverse transcription PCR (RT-PCR).

$35S_{pro}$: DsRed-PTS1 (Zhang and Hu, 2010) was used as the peroxisomal marker in UBC22 localization study. Transgenic plants were generated via floral-dipping transformation of DsRed-PTS1- containing plants with *Agrobacterium tumefaciens* harboring *$35S_{pro}$: GFP-UBC22* fusion gene that contains the full-length CDS of *UBC22*. T_1 generation was screened with kanamycin and the selected plants were subjected to confocal microscopy to observe GFP-UBC22 signals.

Nicotiana tabacum (Tobacco) were grown at 24°C with 70% humidity and white light illumination at 50 μmol m^{-2} s^{-2} for 14 h per day. *A. tumefaciens* cells harboring *$35S_{pro}$: YFP-UBC22* or *$35S_{pro}$: YFP-UBC22ΔKRL* were co-infiltrated with *A. tumefaciens* cells harboring *$35S_{pro}$: DsRed-PTS1*into mature leaves. The infiltrated tobacco plants

were incubated in the same growth condition for another 2 days before subjected to confocal imaging.

2.4.2 RT-PCR

Total RNA was extracted from 2-week-old plants and adult plant flowers using the RNeasy plant mini kit (Qiagen, USA) as instructions. 500 ng of RNA was reverse transcribed using Omniscript RT kit (Qiagen, USA) using oligodT primers. 5 ng of cDNA was used in PCR amplification (Promega, USA) using gene-specific primers.

PCR conditions: 1) 95°C for 2 min, 30 cycles of step 2) – 4), 2) 95°C for 30 sec, 3) 55°C for 30 sec, 4) 72°C for 1min, 5) final extension 72°C for 10 min.

2.4.3 Gene cloning and plasmid construction

CDS of *UBC22* was used in localization study. Sequence was amplified from cDNA that had been reverse transcribed from Col-0 total mRNA. PCR fragments were cloned to a pDonor^{TM}207 then into the pCHF3 vector. Since the GFP signals were lost in T2 plants, I then generated YFP-UBC22 and YFP-UBC22ΔKRL constructs using the binary vector pEarleyGate 104 (Earley *et al.*, 2006).YFP-UBC22ΔKRL has the last 9 nucleotides of the gene (KRL) deleted.

2.4.4 Confocal microscopy analyses

Confocal images for localization were taken by Navneet. Olympus FluoView 1000 CLSM (Olympus, Tokyo, Japan) were used. For UBC22 localization image, 488 nm Argon were used for GFP excitation and 505-530 nm emission filters to acquire GFP signal, also 543nm HeNe were used for excitation of DsRed and 560-615nm emission filters for DsRed signal.

For root imaging, 5-day old seedlings were stained in 10 μg/ml propidium iodide (PI) for one minute, rinsed, then mounted in dH_2O. PI fluorescence signals were visualized by excitation via Kr/Ar 488-nm laser line and detection with a band-pass 570-670 nm emission filter (González-García *et al.*, 2011). Images were processed by the Olympus FV software 4.1 and assembled by ImageJ software.

2.4.5 Sucrose dependence assay

Surface-sterilized Seeds were resuspended in sterile water and stratified at 4°C for 48h under dark condition. Seeds were sown on 1/2MS medium without exogenous Suc or supplemented with 0.5% (w/v) Suc and solidified with 0.8% agar. Plates were placed in light for one hour then transferred to growth chamber and grown vertically in the dark for seven days. *pex4/pex22* were used as the positive control in this experiment. Hypocotyl lengths were measured with a ruler or using ImageJ 1.48 (http://imagej.nih.gov/ij/). Statistical significance was calculated by the Student's T-test

using GraphPad Prism 6, to determine whether there are differences between Col-0 plants and *ubc22* mutants.

2.4.6 IBA resistance assay

Surface-sterilized seeds were resuspended in sterile water and stratified at 4°C for 48h in the dark. Seeds were sown on 1/2MS medium with IBA (0μM, 5μM, 10μM, 15μM, 20μM, 25μM IBA), or 200nM IAA. Plates were placed vertically in growth chamber with continuous light for 7 days. *pex14* was used as the positive control in this experiment. Primary root lengths were measured by ImageJ 1.48. Statistical significance was calculated by the Student's T-test using GraphPad Prism 6.

2.4.7 Sequence alignment and phylogenetic analysis

The amino acid sequences used in this study were obtained from the National Center for Biotechnology Information website (NCBI: http://www.ncbi.nlm.nih.gov/protein), The Arabidopsis Information Resource (TAIR) (www.arabidopsis.org) and UNIPROT (http://www.uniprot.org/). The sequences were then aligned by the Clustal W method and grouped into a phylogenetic tree by MEGA6 software (http://www.megasoftware.net/) (Tamura *et al.*, 2013). MEGA6 was used to generate the neighbor-joining tree and perform bootstrap analysis using the distance analysis function with 1000 replicates.

Amino acid sequences were aligned by ClustalW2 (http://www.ebi.ac.uk/Tools/msa/clustalw2/) and further shaded into graphical format by ESPript 3 software (http://espript.ibcp.fr/ESPript/ESPript/) (Robert and Gouet, 2014).

2.4.8 Pollen viability assay

A simplified Alexander staining method as described in (Peterson *et al.*, 2010) was used in this study. Anthers were removed from open flowers, fixed in Carnoys fixative (6 ethanol: 3 chloroform: 1 glacial acetic acid) for at least two hours, before they were stained by Alexanders staining (10ml 95% ethanol, 25ml glycerol, 1ml Malachite green (1% solution in 95% ethanol), 5ml Acid fuchsin (1% solution in water), 0.5ml Orange G (1% solution in water), 4ml glacial acetic acid, 54.5ml distilled water) buffer on slides. Bottom of the slides were carefully heated with a burner until the stain was completely absorbed into pollen grains. Overheating of the samples should be avoided in this process. Images were taken by Zeiss Axio Imager.M1 microscope (Carl Zeiss).

ACKNOWLEDGEMENTS

We thank the GABI-Kat (Germany) for the T-DNA insertion mutant *ubc22-1*, and ABRC (USA) for the T-DNA insertion mutant *ubc22-2*. We also thank Melinda Frame (Center of Advance Microscopy, MSU) for help with the confocal microscopy, Dr. Weili Yang (MSU) for help with fatty acid analysis. This work was supported by grants to JH from the Chemical Sciences, Geo-sciences and Biosciences Division, Office of Basic

Energy Sciences, Office of Science, U.S. Department of Energy (DE-FG02-91ER20021), and National Science Foundation (MCB 1330441).

REFERENCES

REFERENCES

Alonso-Blanco, C., Blankestijn-de Vries, H., Hanhart, C.J., and Koornneef, M. (1999). Natural allelic variation at seed size loci in relation to other life history traits of Arabidopsis thaliana. Proc. Natl. Acad. Sci. U. S. A. **96**: 4710–7.

Boisson-Dernier, A., Frietsch, S., Kim, T.-H., Dizon, M.B., and Schroeder, J.I. (2008). The peroxin loss-of-function mutation abstinence by mutual consent disrupts male-female gametophyte recognition. Curr. Biol. **18**: 63–8.

Bonnet, J., Devys, D., and Tora, L. (2014). Histone H2B ubiquitination: signaling not scrapping. Drug Discov. Today. Technol. **12**: e19–27.

Van Daele, I., Gonzalez, N., Vercauteren, I., de Smet, L., Inzé, D., Roldán-Ruiz, I., and Vuylsteke, M. (2012). A comparative study of seed yield parameters in Arabidopsis thaliana mutants and transgenics. Plant Biotechnol. J. **10**: 488–500.

Dikic, I., Wakatsuki, S., and Walters, K.J. (2009). Ubiquitin-binding domains - from structures to functions. Nat. Rev. Mol. Cell Biol. **10**: 659–71.

Earley, K.W., Haag, J.R., Pontes, O., Opper, K., Juehne, T., Song, K., and Pikaard, C.S. (2006). Gateway-compatible vectors for plant functional genomics and proteomics. Plant J. **45**: 616–29.

Garcia-Hernandez, M. et al. (2002). TAIR: a resource for integrated Arabidopsis data. Funct. Integr. Genomics **2**: 239–53.

González-García, M.-P., Vilarrasa-Blasi, J., Zhiponova, M., Divol, F., Mora-García, S., Russinova, E., and Caño-Delgado, A.I. (2011). Brassinosteroids control meristem size by promoting cell cycle progression in Arabidopsis roots. Development **138**: 849–59.

Goto, S., Mano, S., Nakamori, C., and Nishimura, M. (2011). Arabidopsis ABERRANT PEROXISOME MORPHOLOGY9 is a peroxin that recruits the PEX1-PEX6 complex to peroxisomes. Plant Cell **23**: 1573–87.

Grou, C.P., Carvalho, a F., Pinto, M.P., Alencastre, I.S., Rodrigues, T. a, Freitas, M.O., Francisco, T., Sá-Miranda, C., and Azevedo, J.E. (2009). The peroxisomal protein import machinery--a case report of transient ubiquitination with a new flavor. Cell. Mol. Life Sci. **66**: 254–62.

Grou, C.P., Carvalho, A.F., Pinto, M.P., Wiese, S., Piechura, H., Meyer, H.E., Warscheid, B., Sá-Miranda, C., and Azevedo, J.E. (2008). Members of the E2D (UbcH5) family mediate the ubiquitination of the conserved cysteine of Pex5p, the peroxisomal import receptor. J. Biol. Chem. **283**: 14190–7.

Hasan, S., Platta, H.W., and Erdmann, R. (2013). Import of proteins into the peroxisomal matrix. Front. Physiol. **4**: 261.

Hicke, L., Schubert, H.L., and Hill, C.P. (2005). Ubiquitin-binding domains. Nat. Rev. Mol. Cell Biol. **6**: 610–21.

Hruz, T., Laule, O., Szabo, G., Wessendorp, F., Bleuler, S., Oertle, L., Widmayer, P., Gruissem, W., and Zimmermann, P. (2008). Genevestigator v3: a reference expression database for the meta-analysis of transcriptomes. Adv. Bioinformatics **2008**: 420747.

Hu, J., Baker, A., Bartel, B., Linka, N., Mullen, R.T., Reumann, S., and Zolman, B.K. (2012). Plant peroxisomes: biogenesis and function. Plant Cell **24**: 2279–303.

Hua, Y. and Chua, N.-H. (2003). The Arabidopsis Auxin-Inducible Gene ARGOS Controls Lateral. Plant Cell **15**: 1951–1961.

Hua, Z. and Vierstra, R.D. (2011). The cullin-RING ubiquitin-protein ligases. Annu. Rev. Plant Biol. **62**: 299–334.

Hurley, J.H., Lee, S., and Prag, G. (2006). Ubiquitin-binding domains. Biochem. J. **399**: 361–72.

Kiel, J. a. K.W., Emmrich, K., Meyer, H.E., and Kunau, W.-H. (2004). Ubiquitination of the Peroxisomal Targeting Signal Type 1 Receptor, Pex5p, Suggests the Presence of a Quality Control Mechanism during Peroxisomal Matrix Protein Import. J. Biol. Chem. **280**: 1921–1930.

Kleinboelting, N., Huep, G., Kloetgen, A., Viehoever, P., and Weisshaar, B. (2012). GABI-Kat SimpleSearch: new features of the Arabidopsis thaliana T-DNA mutant database. Nucleic Acids Res. **40**: D1211–5.

Kraft, E., Stone, S.L., Ma, L., Su, N., Gao, Y., Lau, O., Deng, X., and Callis, J. (2005). Genome Analysis and Functional Characterization of the E2 and RING-Type E3 Ligase Ubiquitination Enzymes of Arabidopsis 1 [W]. Genome Anal. **139**: 1597–1611.

Kragt, A., Voorn-Brouwer, T., van den Berg, M., and Distel, B. (2005). The Saccharomyces cerevisiae peroxisomal import receptor Pex5p is monoubiquitinated in wild type cells. J. Biol. Chem. **280**: 7867–74.

Krogh, a, Larsson, B., von Heijne, G., and Sonnhammer, E.L. (2001). Predicting transmembrane protein topology with a hidden Markov model: application to complete genomes. J. Mol. Biol. **305**: 567–80.

Li, X.-R., Li, H.-J., Yuan, L., Liu, M., Shi, D.-Q., Liu, J., and Yang, W.-C. (2014). Arabidopsis DAYU/ABERRANT PEROXISOME MORPHOLOGY9 Is a Key Regulator of Peroxisome Biogenesis and Plays Critical Roles during Pollen Maturation and Germination in Planta. Plant Cell: 1–18.

Lingner, T., Kataya, A.R., Antonicelli, G.E., Benichou, A., Nilssen, K., Chen, X.-Y., Siemsen, T., Morgenstern, B., Meinicke, P., and Reumann, S. (2011). Identification of novel plant peroxisomal targeting signals by a combination of machine learning methods and in vivo subcellular targeting analyses. Plant Cell **23**: 1556–72.

Okumoto, K., Misono, S., Miyata, N., Matsumoto, Y., Mukai, S., and Fujiki, Y. (2011). Cysteine ubiquitination of PTS1 receptor Pex5p regulates Pex5p recycling. Traffic **12**: 1067–83.

Peterson, R., Slovin, J.P., and Chen, C. (2010). A simplified method for differential staining of aborted and non-aborted pollen grains. Int. J. Plant Biol. **1**.

Platta, H.W., El Magraoui, F., Schlee, D., Grunau, S., Girzalsky, W., and Erdmann, R. (2007). Ubiquitination of the peroxisomal import receptor Pex5p is required for its recycling. J. Cell Biol. **177**: 197–204.

Robert, X. and Gouet, P. (2014). Deciphering key features in protein structures with the new ENDscript server. Nucleic Acids Res. **42**: W320–4.

Schrader, M. and Fahimi, H.D. (2008). The peroxisome: still a mysterious organelle. Histochem. Cell Biol. **129**: 421–40.

Schwacke, R., Schneider, A., Graaff, E. Van Der, Fischer, K., Catoni, E., Desimone, M., Frommer, W.B., Flu, U., Kunze, R., and Germany, E.C. (2003). ARAMEMNON , a Novel Database for Arabidopsis Integral Membrane Proteins 1. Genome Anal. **131**: 16–26.

Skowyra, D., Koepp, D.M., Kamura, T., Conrad, M.N., Conaway, R.C., Conaway, J.W., Elledge, S.J., and Harper, J.W. (1999). Reconstitution of G1 Cyclin Ubiquitination with Complexes Containing SCFGrr1 and Rbx1. Science (80-.). **284**: 662–665.

Takahashi, H., Nozawa, A., Seki, M., Shinozaki, K., Endo, Y., and Sawasaki, T. (2009). A simple and high-sensitivity method for analysis of ubiquitination and polyubiquitination based on wheat cell-free protein synthesis. BMC Plant Biol. **9**: 39.

Tamura, K., Stecher, G., Peterson, D., Filipski, A., and Kumar, S. (2013). MEGA6: Molecular Evolutionary Genetics Analysis version 6.0. Mol. Biol. Evol. **30**: 2725–9.

Varshavsky, A. (2012). The ubiquitin system, an immense realm. Annu. Rev. Biochem. **81**: 167–76.

Welsh, J.B., Zarrinkar, P.P., Sapinoso, L.M., Kern, S.G., Behling, C. a, Monk, B.J., Lockhart, D.J., Burger, R. a, and Hampton, G.M. (2001). Analysis of gene expression profiles in normal and neoplastic ovarian tissue samples identifies candidate molecular markers of epithelial ovarian cancer. Proc. Natl. Acad. Sci. U. S. A. **98**: 1176–81.

Van Wijk, S.J.L. and Timmers, H.T.M. (2010). The family of ubiquitin-conjugating enzymes (E2s): deciding between life and death of proteins. FASEB J. **24**: 981–93.

Zhang, X. and Hu, J. (2010). The Arabidopsis chloroplast division protein DYNAMIN-RELATED PROTEIN5B also mediates peroxisome division. Plant Cell **22**: 431–42.

Zolman, B.K. and Bartel, B. (2004). An Arabidopsis indole-3-butyric acid-response mutant defective in PEROXIN6, an apparent ATPase implicated in peroxisomal function. Proc. Natl. Acad. Sci. U. S. A. **101**: 1786–91.

Zolman, B.K., Monroe-Augustus, M., Thompson, B., Hawes, J.W., Krukenberg, K. a, Matsuda, S.P., and Bartel, B. (2001). chy1, an Arabidopsis mutant with impaired beta-oxidation, is defective in a peroxisomal beta-hydroxyisobutyryl-CoA hydrolase. J. Biol. Chem. **276**: 31037–46.

Zolman, B.K., Yoder, a, and Bartel, B. (2000). Genetic analysis of indole-3-butyric acid responses in Arabidopsis thaliana reveals four mutant classes. Genetics **156**: 1323–37.